NATURAL FREQUENCIES OF NON-UNIFORM BEAMS

by

Thomas J. Ballen, Jr.

A Thesis Submitted to the Faculty of the

DEPARTMENT OF CIVIL ENGINEERING

In Partial Fulfillment of the Requirements
For the Degree of

MASTER OF SCIENCE

In the Graduate College

THE UNIVERSITY OF ARIZONA

1 9 6 4

STATEMENT BY AUTHOR

This thesis has been submitted in partial fulfillment of requirements for an advanced degree at The University of Arizona and is deposited in The University Library to be made available to borrowers under rules of the Library.

Brief quotations from this thesis are allowable without special permission, provided that accurate acknowledgment of source is made. Requests for permission for extended quotation from or reproduction of this manuscript in whole or in part may be granted by the head of the major department or the Dean of the Graduate College when in their judgment the proposed use of the material is in the interests of scholarship. In all other instances, however, permission must be obtained from the author.

SIGNED: Thomas J. Ballen, Jr.

APPROVAL BY THESIS DIRECTOR

This thesis has been approved on the date shown below:

Morris W. Self
M.W. SELF
Associate Professor of Civil Engineering

May 5, 1964
Date

ACKNOWLEDGEMENT

I wish to thank Dr. Donald DaDeppo for his inspiration and guidance, not only in this thesis, but during the entirety of my graduate studies. Thanks also to Dr. M.W. Self, who in the final stages provided council and aid and the much-needed "let's get it done" atmosphere.

And last, but never least, grateful thanks to my wife who typed her way through a text which was literally 'greek'.

T.J. Ballen

NOTATION

A - cross-sectional area

B - constant

C - constant

D - determinant of coefficients

E - modulus of elasticity

F - transcendental function of p

G - defined as $\int_0^1 \rho \phi_i^2 \, d\eta = G_i$

I - moment of inertia

K - constant

L - constant

M - moment at a given section

N - $N(x) = \sum_{i=1}^{\infty} a_i \phi_i$

Q - function in the Rayleigh-Ritz solution

T - harmonic function

V - shear at a given section

Y - normal function

a - constant

b - ratio of constants

f - transcendental function of η and p k - constant

l - length

p - numerical variable

t - time

w - forcing function

x - rectangular coordinate

y - rectangular coordinate

η - dimensionless length parameter

μ - mass density

ρ - dimensionless area function

τ - depth ratio: h_1/h_0 ; $h_1 > h_0$

ϕ - natural mode of vibration

ψ - dimensionless moment of inertia function

ω - natural frequency

TABLE OF CONTENTS

INTRODUCTION

The problem to be considered in this thesis is that of transverse vibrations of beams of variable cross-section. A linear small-deflection theory is utilized for the solution.

Because the linear small-deflection theory has long been well developed, many attempts have been made to solve the the transverse vibration problem for beams of variable cross-section. In fact exact solutions for specific cross-sectional forms have been obtained [(1,3,10)*]. Unfortunately, the governing differential equation for the transverse vibration problem is not conducive to rapid or exact solution even when shear and rotary inertia effects are neglected. Consequently, most of the exact solutions thus far generated are for somewhat unrealistic variations in cross-section.

In order to obtain solutions for cross-sections commonly encountered in structural engineering, one is virtually forced to use approximate methods of solution. Certain approximate solutions have been obtained for the natural frequencies and mode shapes by the use of the Rayleigh-Ritz method [(7)], by replacing the continuous

---

* Numbers refer to references in the Bibliography.

system by a "lumped-parameter" system [2,4], and by finite difference techniques [5].

This thesis is concerned with the determination of the low order natural frequencies and mode shapes for simply-supported beams with constant width and depths which vary linearly and parabolically along the length of the beam. Solutions are obtained by the Rayleigh-Ritz method. In applying the Rayleigh-Ritz method, the mode shapes for the specific beam are expanded in an infinite series. Substitution of this series into the Rayleigh-Ritz equations yields an infinite set of equations, the terms of which are expanded in terms of infinite series, to be solved for the natural frequencies and the constants which define the corresponding mode shapes.

NEGLECTED PHENOMENA

Before proceeding to the analysis, it must be noted that the effects of shear, rotary inertia, and damping are omitted in this thesis.

Omission of the above factors is necessary in order to obtain a relatively simple governing equation, which though simplified yet reflects the principle features of the problem, ie., the variation of mass and stiffness of the beam. It is not, however, unreasonable to omit consideration of shear, rotary inertia, and damping when the beam is relatively long and the damping effect is small.(12)

For the case of the uniform simply-supported beam, the shear distortion and rotary inertia affect only the natural frequencies. On the basis of energy considerations, it can be shown that the effect of both shear and rotary inertia is to reduce the natural frequencies.

For other than the short and stubby beam, the effects of shear and rotary inertia are only appreciable in cases of relatively short wave lengths, ie., in the higher modes of vibration.(12)

In general damping has a two-fold effect on the vibration characteristics of a linear system. Damping, first tends to reduce the frequency of vibration, and second, tends to distort, ie. change, the mode shapes. The extent to which the frequencies and mode shapes are changed is in effect a measure of the damping.

DERIVATION OF THE EQUATIONS OF MOTION

In the derivation of the equations of motion which follows, these listed assumptions are made:

1. The beam under consideration is long and slender, such that any cross-sectional dimension is very small when compared to the beam length.
2. There is linear elastic behavior throughout.
3. The beam has a plane of symmetry, and the vibration occurs in this plane.
4. The oscillations are so small that the use of small angle geometry is valid.
5. Plane sections remain plane.
6. Strain in the transverse direction is zero.
7. There is no damping.

Considering the foregoing assumptions, it is possible; without inducing appreciable error, to ignore the effects of shear and rotary inertia.

The equations of motion are derived for a beam (Fig. 1)

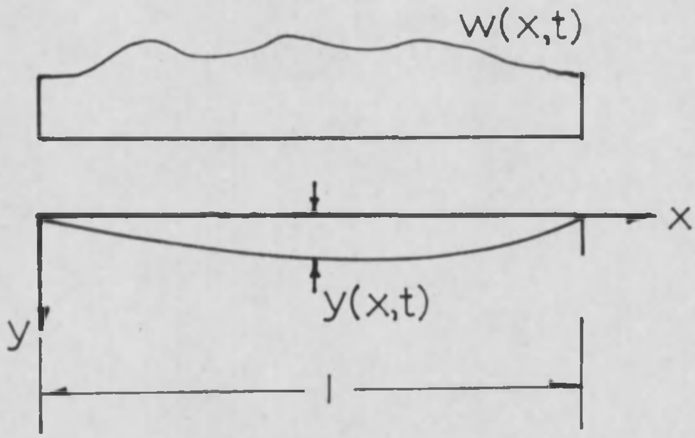

Fig. 1

of length l, having a cross-sectional area $A = A_o\rho(x)$, a moment of inertia $I = I_o\psi(x)$, a constant modulus of elasticity E, and a constant mass density μ.

The functions $\rho(x)$ and $\psi(x)$ are dimensionless functions of the length-measuring co-ordinate x, and A_o and I_o are the area and moment of inertia respectively at some suitably chosen section of the beam.

To derive the equations of motion, consider a differential element of the beam (Fig. 2) acted on by a forcing function $w = w(x,t)$.

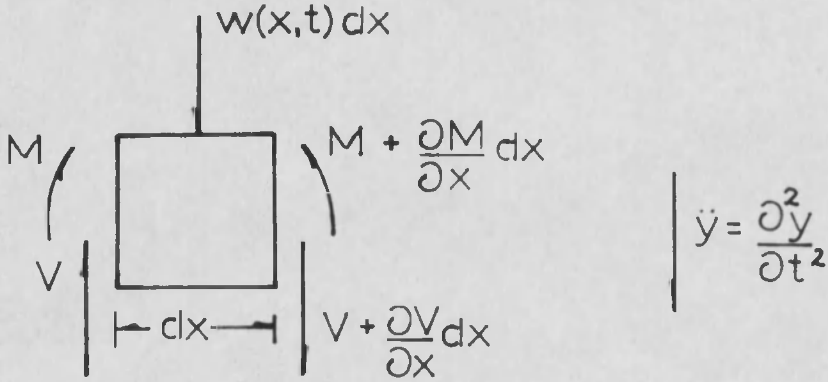

Fig. 2

Applying D'Alembert's Principle and considering equilibrium

$$\Sigma F_v = 0$$

$$\mu A_o \rho(x) \frac{\partial^2 y}{\partial t^2} dx - V - \frac{\partial V}{\partial x} dx + V - w(x,t) dx = 0$$

$$\mu A_o \rho(x) \frac{\partial^2 y}{\partial t^2} = \frac{\partial V}{\partial x} + w(x,t) \qquad \text{or}$$

$$\frac{\partial V}{\partial x} = \mu A_o \rho(x) \frac{\partial^2 y}{\partial t^2} - w(x,t) \tag{1}$$

$$\Sigma M = 0$$

$$M - M - \frac{\partial M}{\partial x} dx + V dx + \frac{\partial V}{\partial x} (dx)^2 +$$

$$w(x,t)\, dx \cdot \frac{dx}{2} + \mu A_o \rho(x)\, dx \cdot \frac{dx}{2} = 0$$

and dividing by dx and passing to the limit

$$V = \frac{\partial M}{\partial x} \tag{2}$$

Considering the assumptions previously stated, the deflection curve of the beam may be represented by the differential equation

$$-M = EI\frac{\partial^2 y}{\partial x^2} \tag{3}$$

and substituting values from equations (1) and (2) in equation (3)

$$EI_o\frac{\partial^2}{\partial x^2}\left[\psi(x)\frac{\partial^2 y}{\partial x^2}\right] + \mu A_o\rho(x)\frac{\partial^2 y}{\partial t^2} = w(x,t) \tag{4}$$

which is the differential equation of motion for the beam acted upon by the forcing function w.

For free vibration the equation of motion reduces to

$$EI_o\frac{\partial^2}{\partial x^2}\left[\psi(x)\frac{\partial^2 y}{\partial x^2}\right] + \mu A_o\rho(x)\frac{\partial^2 y}{\partial t^2} = 0 \tag{5}$$

It is convenient to introduce a dimensionless length parameter η, defined as

$$\eta = \frac{x}{l} \tag{6}$$

Substituting equation (6) in equation (5) and denoting differentiation with respect to η by primes and with respect to time by dots gives

$$\frac{1}{\rho(\eta l)}\left[\psi(\eta l)\, y''\right]'' + \frac{\mu A_o l^4}{EI_o}\ddot{y} = 0 \tag{7}$$

A constant k is defined as

$$k^4 = \frac{\mu A_o l^4}{EI_o} \tag{8}$$

The dimensionless differential equation of motion becomes

$$\frac{1}{\rho}\left[\psi y''\right]'' + k^4\ddot{y} = 0 \tag{9}$$

Equation (9) can be solved by the separation of variables by letting

$$y = Y(\eta) \cdot T(t) \tag{10}$$

where Y is the normal function, a function of η alone; and T is the harmonic function, a function of time alone.

Substituting equation (10) in equation (9), and separating the variables yields

$$\frac{1}{\rho Y}\left[\psi Y''\right]'' = -k^4 \frac{\ddot{T}}{T} \tag{11}$$

which can be satisfied for all time and all η , if and only if each side of equation (11) is respectively equal to a constant which is denoted as p^4. Therefore, equation (11) may be divided into two parts:

1. $$p^4 = -k^4 \frac{\ddot{T}}{T} \quad \text{and} \tag{12}$$

2. $$p^4 = \frac{1}{\rho Y}\left[\psi Y''\right]'' \tag{13}$$

Writing equation (12) in standard form and letting the natural circular frequency

$$\omega = \left(\frac{p}{k}\right)^2 \tag{14}$$

we find

$$\ddot{T} + \omega^2 T = 0 \tag{15}$$

the solution of which is well known as

$$T = B \sin \omega t + C \cos \omega t \tag{16}$$

where B and C are constants to be determined from initial conditions.

Substituting the value of k^4 from equation (8) in equation (14), the square of the natural frequency ω^2 is

$$\omega^2 = \frac{p^4 EI_o}{\mu A_o l^4} \tag{17}$$

Letting the constant,

$$\omega' = \frac{\pi^2}{l^2} \sqrt{\frac{EI_o}{\mu A_o}} \tag{18}$$

the natural frequency ω becomes

$$\omega = \frac{p^2 \omega'}{\pi^2} \tag{19}$$

The second part of the equation of motion, equation (13), when written in standard form is

$$\left[\psi Y''\right]'' - \rho p^4 Y = 0 \tag{20}$$

which is a linear, homogeneous, fourth order differential equation with variable coefficients, the solution of which is of the general form

$$Y = a_1 f_1(\eta, p) + a_2 f_2(\eta, p) + a_3 f_3(\eta, p) + a_4 f_4(\eta, p) \tag{21}$$

where the f_i's are transcendental functions of η and p and where the a_i's are constants to be determined from the boundary conditions.

The most common boundary conditions encountered are the clamped, free, and simply supported end. The boundary conditions of each being homogeneous and of the form:

1. Clamped: $y = 0;\ y' = 0$ (22a)
2. Free: $EIy'' = 0;\ (EIy'')' = 0$ (22b)
3. Simply Supported: $y = 0;\ EIy'' = 0$ (22c)

Any combination of the boundary conditions, equations (22), when substituted in equation (21) yields four, linear, homogeneous simultaneous equations to be solved for the a_i's of the form

$$a_1 F_{11}(p) + a_2 F_{12}(p) + a_3 F_{13}(p) + a_4 F_{14}(p) = 0 \qquad (23a)$$

$$a_1 F_{21}(p) + a_2 F_{22}(p) + a_3 F_{23}(p) + a_4 F_{24}(p) = 0 \qquad (23b)$$

$$a_1 F_{31}(p) + a_2 F_{32}(p) + a_3 F_{33}(p) + a_4 F_{34}(p) = 0 \qquad (23c)$$

$$a_1 F_{41}(p) + a_2 F_{42}(p) + a_3 F_{43}(p) + a_4 F_{44}(p) = 0 \qquad (23d)$$

where the F_{ij}'s are transcendental functions of p.

In order to obtain a non-trivial solution for the constants a_i, the determinant D(p) of the coefficients of the a_i's must be zero, ie.

$$\begin{vmatrix} F_{11} & F_{12} & F_{13} & F_{14} \\ F_{21} & F_{22} & F_{23} & F_{24} \\ F_{31} & F_{32} & F_{33} & F_{34} \\ F_{41} & F_{42} & F_{43} & F_{44} \end{vmatrix} = \left| F_{ij} \right| = D(p) = 0 \qquad (24)$$

Expansion of the determinant, equation (24), leads to a single transcendental equation to be solved for the parameter p. This single equation is commonly referred to as the frequency equation. In general there will be an infinite number of p's which are roots of the frequency equation and which will define the natural frequencies of vibration through equation (19).

Upon substitution of a particular value of p in equations (23) there then exists four, homogeneous simultaneous equations to be solved for the particular a_i constants. But of the four equations, only three are independent. Thus it is only possible to determine three of the constants in terms of the fourth.

The ratios b_{ns} are defined as:

$$b_{2s} = \frac{a_{2s}}{a_{1s}} \tag{25a}$$

$$b_{3s} = \frac{a_{3s}}{a_{1s}} \quad \text{and} \tag{25b}$$

$$b_{4s} = \frac{a_{4s}}{a_{1s}} \tag{25c}$$

where the subscript numbers denote the appropriate constant, and the subscript letter s denotes the appropriate s root

(p_s) of the frequency equation.

Upon substitution of b_{ns} and a_{1s} into equation (21) the normal function Y becomes

$$Y_s = a_{1s}\,[\,f_1(\eta,p) + b_{2s}f_2(\eta,p) + b_{3s}f_3(\eta,p) + b_{4s}f_4(\eta,p)] \qquad (26)$$

The normal mode shapes ϕ are defined as

$$\phi_s(\eta) = f_1(\eta,p) + b_{2s}f_2(\eta,p) + b_{3s}f_3(\eta,p) + b_{4s}f_4(\eta,p) \qquad (27)$$

where $\phi_s(\eta)$ is the normal mode of vibration compatible with the s th root of the frequency equation and which satisfies the prevailing geometric boundary conditions.

The normal function Y_s is now expressible as

$$Y_s = a_{1s} \cdot \phi_s(\eta) \qquad (28)$$

Substituting the values of Y_s and T into equation (10) gives

$$y_s = a_{1s}\,\phi_s(\eta)\,[\,B \sin\omega_s t + C \cos\omega_s t] \qquad (29)$$

or

$$y_s = \phi_s(\eta)\,[K_s \sin \omega_s t + L_s \cos \omega_s t] \qquad (30)$$

For a linear differential equation, the total solution is a linear combination of all the elementary solutions. The total solution for the deflection y, therefore, becomes

$$y = \sum_{s=1}^{\infty} \phi_s(\eta)\left[K_s \sin \omega_s t + L_s \cos \omega_s t\right] \qquad (31)$$

ORTHOGONALITY CONDITIONS

For future considerations, it is advantageous to develop the orthogonality conditions of the mode shapes.

Considering specific values of Y, the differential equations defining Y_i and Y_j may be written as

$$\left(\psi Y_i''\right)'' - \rho p_i^4 Y_i = 0 \quad \text{and} \tag{32}$$

$$\left(\psi Y_j''\right)'' - \rho p_j^4 Y_j = 0 \tag{33}$$

Replacing the Y's by their values in terms of the mode shapes equations (32) and (33) become

$$\left(\psi \phi_i''\right)'' - \rho p_i^4 \phi_i = 0 \quad \text{and} \tag{34}$$

$$\left(\psi \phi_j''\right)'' - \rho p_j^4 \phi_j = 0 \tag{35}$$

Multiplying equation (34) by ϕ_j, equation (35) by ϕ_i, and subtracting gives

$$\left[\psi \phi_i''\right]'' \phi_j - \left[\psi \phi_j''\right]'' \phi_i -$$

$$\rho(p_i^4 - p_j^4)\phi_i \phi_j = 0 \tag{36}$$

Integrating equation (36) over the beam length yields

$$\int_0^1 \left\{\left[\psi \phi_i''\right]'' \phi_j - \left[\psi \phi_j''\right]'' \phi_i\right\} d\eta =$$

$$(p_i^4 - p_j^4) \int_0^1 \rho \phi_i \phi_j \, d\eta \tag{37}$$

The left side of equation (37) when integrated by parts becomes

$$\left\{\phi_j\left[\psi \phi_i''\right]' - \phi_j'\left[\psi \phi_i''\right] - \phi_i\left[\psi \phi_j''\right]' + \phi_i'\left[\psi \phi_j''\right]\right\}\Bigg|_0^1 \tag{38}$$

After rewriting the boundary conditions, equations (22), in terms of the mode shapes,

1. Clamped: $\phi_i = 0$ $\qquad \phi_i' = 0$ (39a)
2. Free: $EI\phi_i'' = 0$ $\qquad (EI\phi_i'')' = 0$ (39b)
3. Simply Supported: $\phi_i = 0$ $\qquad EI\phi_i'' = 0$ (39c)

it is apparent that for any combination of the common boundary conditions, equations (39), that the respective terms of (38), when evaluated at the indicated limits, will always be zero for i different than j. And since p_i does not equal p_j *

$$\int_0^1 \rho \phi_i \phi_j \, d\eta = 0 \quad \text{and} \tag{40}$$

$$\int_0^1 \left[(\psi \phi_i'')'' \phi_j - (\psi \phi_j'')'' \phi_i \right] d\eta = 0 \tag{41}$$

The orthogonality conditions are obtained by multiplying equation (34) by ϕ_j; and integrating over the beam length.

* p's are assumed to be distinct.

$$\int_0^1 [\psi \phi_i'']'' \phi_j \, d\eta \; - \; p_i^4 \int_0^1 \rho \phi_i \phi_j \, d\eta \; = \; 0 \qquad (42)$$

But from equation (40), equation (42) reduces to

$$\int_0^1 [\psi \phi_i'']'' \phi_j \, d\eta \; = \; 0 \qquad (43)$$

and the orthogonality conditions may be written in the form

$$\int_0^1 \rho \phi_i \phi_j \, d\eta \; = \; 0 \qquad \text{and} \qquad (44)$$

$$\int_0^1 [\psi \phi_i'']'' \phi_j \, d\eta \; = \; 0 \qquad (45)$$

for i different than j.

When i equals j, equations (34) and (35) become identical. Multiplying equation (34) by ϕ_i and integrating over the beam length yields

$$\int_0^1 [\psi \phi_i'']'' \phi_i \, d\eta \; = \; p_i^4 \int_0^1 \rho \phi_i^2 \, d\eta \qquad (46)$$

Integrating the left side of equation (46) and regarding only the first two terms of this integration gives

$$\left\{ \phi_i \left[\psi \phi_i'' \right]' - \phi_i' \left[\psi \phi_i'' \right] \right\} \Bigg|_0^1 \tag{47}$$

Considering the boundary conditions, equations (39), it is evident that (47), when evaluated at the designated limits, will be zero. Therefore,

$$\int_0^1 \psi \phi_i''^2 d\eta = p_i^4 \int_0^1 \rho \phi_i^2 d\eta \tag{48}$$

For future use, it is convenient to define

$$G_i = \int_0^1 \rho \phi_i^2 d\eta \tag{49}$$

Given initial conditions appropriate for a given problem, it is possible, by using the orthogonality conditions stipulated in equations (44) and (45), to evaluate the constants K_s and L_s of equation (31).

Multiplying equation (31) by $\rho\phi_i$ and integrating over the beam length gives

$$\int_0^1 \rho y \phi_i \, d\eta = \int_0^1 \sum_{s=1}^{\infty} \rho \phi_i \phi_s \left[K_s \sin \omega_s t + L_s \cos \omega_s t \right] d\eta \tag{50}$$

Assuming that the integration and summation may be interchanged and using the orthogonality conditions, the right side of equation (50) will be non-zero only when s is equal to i. Therefore,

$$\int_0^1 \rho y \phi_i \, d\eta = \left[K_i \sin \omega_i t + L_i \cos \omega_i t \right] \left(\int_0^1 \rho \phi_i^2 \, d\eta \right) \tag{51}$$

Assuming initial conditions of the form:

1. $y(x,0) = y_o$ (52a)
2. $\dot{y}(x,0) = \dot{y}_o$ (52b)

and utilizing the results of equation (49), the constants K_i and L_i may be calculated from

$$K_i = \frac{1}{G_i \omega_i} \int_0^1 \rho \phi_i \dot{y}_o \, d\eta \tag{53}$$

$$L_i = \frac{1}{G_i} \int_0^1 \rho \phi_i y_o \, d\eta \tag{54}$$

SIMPLY SUPPORTED BEAM - CONSTANT A AND I

To demonstrate how an exact solution is obtained, a beam of constant A and I, ie. $\rho(\eta) = 1 = \psi(\eta)$, is considered.

The harmonic function remains as

$$T = B \sin \omega t + C \cos \omega t \tag{16}$$

but the differential equation defining the normal function is now

$$Y'''' - p^4 Y = 0 \tag{55}$$

the solution of which defines the transcendental functions f_i and gives

$$\begin{aligned} Y = {} & a_1 \sin p\eta + a_2 \cos p\eta + a_3 \sinh p\eta \\ & + a_4 \cosh p\eta \end{aligned} \tag{56}$$

Substitution of equation (56) in the boundary conditions for a simply supported beam yields:

$$\begin{array}{rcccl} 0 & + a_2 & + 0 & + a_4 & = 0 \\ 0 & - a_2 & + 0 & + a_4 & = 0 \\ a_1 \sin p & + a_2 \cos p & + a_3 \sinh p & + a_4 \cosh p & = 0 \\ - a_1 \sin p & - a_2 \cos p & + a_3 \sinh p & + a_4 \cosh p & = 0 \end{array} \tag{57}$$

from which a_2, a_3, and a_4 equal zero, and

$$a_1 \sin p = 0 \tag{58}$$

For a non-trivial solution of equation (58)

$$p = n\pi \tag{59}$$

The n th natural frequency then is

$$\omega_n = n^2\omega' \tag{60}$$

and the corresponding mode shape is

$$\phi_n = \sin n\pi\eta \tag{61}$$

The deflection curve y becomes

$$y = \sum_{n=1}^{\infty} \sin n\pi\eta \left[K_n \sin n^2\omega' t + L_n \cos n^2\omega' t\right] \tag{62}$$

and

$$G_n = \int_0^1 \sin^2 n\pi\eta \, d\eta = \frac{1}{2} \tag{63}$$

The coefficients K_n and L_n depend on the specific prescribed initial conditions, and may be calculated from

$$K_n = \frac{2}{n^2\omega'}\int_0^1 \dot{y}_0 \sin n\pi\eta \, d\eta \quad \text{and} \tag{64}$$

$$L_n = 2\int_0^1 y_0 \sin n\pi\eta \, d\eta \tag{65}$$

RAYLEIGH-RITZ SOLUTION

It is apparent that the exact solution of the problem depends upon the ability of ascertaining the mode shapes.

Because the differential equation defining the mode shapes, equation (34), is virtually impossible to solve exactly for realistic distributions of mass and stiffness, approximate methods of solution must be used.

The approximate method used in this thesis is the Rayleigh-Ritz method. The mode shapes of the non-uniform beam are expanded in an infinite series, and Rayleigh's Principle is used to derive an infinite set of equations - the Rayleigh-Ritz equations - to be solved for the natural frequencies and the series expansion coefficients which define the corresponding mode shapes.

The Rayleigh-Ritz equations are developed from energy considerations. It is assumed that ideal frictionless constraints are imposed on the beam such that the beam is forced to vibrate as a single degree of freedom system. During free vibration the deflection curve of the constrained beam may be expressed as

$$y = N(x) \cdot T(t) \tag{66}$$

where N(x) is determined by the constraints which have been imposed. For this thesis it is assumed that N(x) satisfies the boundary conditions of the unconstrained non-uniform beam and that N(x) is a smooth function which can be expressed as a linear combination of the mode shapes of the unconstrained non-uniform beam in the form

$$N(x) = \sum_{i=1}^{\infty} a_i \phi_i \tag{67}$$

These restrictions on N(x) are not particularly severe.

The harmonic function T(t) for a single degree of freedom is

$$T(t) = A \sin(\omega t + \alpha) \tag{68}$$

For a conservative single degree of freedom system, the natural frequency is determined by equating the maximum potential energy to the maximum kinetic energy. These maximum energies are written as:

1. Potential Energy:

$$PE_{max} = \frac{1}{2}\int_0^l EI {y''}_{max}^2 \, dx \tag{69}$$

2. Kinetic Energy: $$KE_{max} = \frac{1}{2}\int_0^l m\dot{y}_{max}^2 dx \qquad (70)$$

With y and T(t) being defined by equations (66) and (68) respectively, the maximized derivatives appearing in the potential and kinetic energies are

$$y''\ max = AN''(x) \quad \text{and} \qquad (71)$$

$$\dot{y}\ max = A\omega N(x) \qquad (72)$$

Substituting equations (71) and (72) in equations (69) and (70) respectively, equating the maximum energies, and solving for the square of the natural frequency gives

$$\omega^2 = \frac{\int_0^l EI\, N''^2(x)\, dx}{\int_0^l m\, N^2(x)\, dx} \qquad (73)$$

The right side of equation (73) is referred to as the Rayleigh Quotient.

The Rayleigh Quotient indicates for a given beam that the natural frequency ω is a function of the N(x) function.

If a random configuration of vibration is chosen, ie., a random value of N(x) is chosen, the Rayleigh Quotient yields the natural frequency of vibration consistent with the chosen random configuration.

If N(x) is chosen in particular to be proportional to one of the mode shapes ϕ_j of the unconstrained non-uniform system, equation (73) will define a natural frequency ω equal to ω_j , and this ω_j will be stationary. The fact that ω is stationary when N(x) is proportional to one of the mode shapes can be verified by treating ω as a function of N(x) and applying the methods of the calculus of variations to equation (73).

For further calculations it is convenient to expand the mode shapes ϕ_i in an infinite series of the form

$$\phi_i = \sum_{j=1}^{\infty} b_j \bar{\phi}_j \tag{74}$$

where the $\bar{\phi}_j$'s form a complete set of functions, chosen to satisfy the geometric boundary conditions. The expansion coefficients b_j are so chosen to guarantee upon substitution of the infinite series, equation (74), in the Rayleigh Quotient, equation (73), for the N(x) terms, that the generated natural frequency will be stationary.

When the infinite series, equation (74), is substituted in the Rayleigh Quotient, equation (73), for the N(x) functions and the summation and integration are interchanged, equation (73) becomes

$$\omega^2 = \frac{\sum_{j,k=1}^{\infty} b_j b_k \int_0^1 EI \bar{\phi}_j'' \bar{\phi}_k'' dx}{\sum_{j,k=1}^{\infty} b_j b_k \int_0^1 m \bar{\phi}_j \bar{\phi}_k dx} \tag{75}$$

The condition that the square of the natural frequency ω^2 be stationary requires that

$$\delta(\omega^2) = \sum_{l=1}^{\infty} \frac{\partial(\omega^2)}{\partial b_l} \cdot \delta b_l = 0 \tag{76}$$

for all δb_l, and therefore,

$$\frac{\partial(\omega^2)}{\partial b_l} = 0 \quad ; \tag{77}$$

$$l = 1, 2, 3, \ldots \infty$$

If equation (75) is written as

$$\omega^2 = \frac{Q_1}{Q_2} \tag{78}$$

where

$$Q_1 = \sum_{j,k=1}^{\infty} b_j b_k \int_0^1 EI\, \bar{\phi}_j'' \bar{\phi}_k''\, dx \quad \text{and} \tag{79}$$

$$Q_2 = \sum_{j,k=1}^{\infty} b_j b_k \int_0^1 m\, \bar{\phi}_j \bar{\phi}_k\, dx \tag{80}$$

and the square of the natural frequency ω^2 is partially differentiated with respect to b_ℓ, equation (77) reduces to

$$\omega^2 \frac{\partial Q_2}{\partial b_\ell} - \frac{\partial Q_1}{\partial b_\ell} = 0 \tag{81}$$

$$1 = 1, 2, 3, \ldots \infty$$

Differentiating equations (79) and (80) with respect to b_ℓ and substituting in equation (81) gives

$$\omega^2 \sum_{k=1}^{\infty} c_{ik} b_k - \sum_{k=1}^{\infty} d_{ik} b_k = 0 \tag{82}$$

$$i = 1, 2, 3, \ldots \infty$$

where

$$c_{ik} = c_{ki} = \int_0^1 m \bar{\phi}_i \bar{\phi}_k \, dx \quad \text{and} \tag{83}$$

$$d_{ik} = d_{ki} = \int_0^1 EI \bar{\phi}_i'' \bar{\phi}_k'' \, dx \tag{84}$$

The infinite set of homogeneous equations, equations (82), are the Rayleigh - Ritz equations. The solution of the infinite set of equations yields the natural frequencies ω^2, and the coefficients b_k which when substituted in equation (74) yield the mode shapes. In principle, the solution for the mode shapes is exact. An approximation arises when only a finite number of equations (82) are considered.

Because the Rayleigh - Ritz equations are homogeneous, non-trivial solutions for the b_K's exist only when ω takes on particular values. These particular values of ω are the natural frequencies of the beam.

If a value of the natural frequency is designated as ω_i and the corresponding b's are designated as b_K^i , then the Rayleigh - Ritz equations and the mode shape equations are more properly written as

$$\omega_i^2 \sum_{K=1}^{\infty} c_{IK} b_K^i - \sum_{K=1}^{\infty} d_{IK} b_K^i = 0 \quad \text{and} \qquad (85)$$

$$I = 1, 2, 3, \ldots \infty$$

$$\phi_i = \sum_{K=1}^{\infty} b_K^i \bar{\phi}_K \quad \text{where} \qquad (86)$$

$$i = 1, 2, 3, \ldots \infty$$

Using the technique of R.P.N. Jones and S. Malalingem [7], it is convenient to choose the $\bar{\phi}$ functions to be the mode shapes of a uniform beam which has the same boundary conditions as the non-uniform beam.

Jones[7] further states that if the mass and inertia of the non-uniform system vary only slightly from the uniform system, the coefficients c_{ik} and d_{ik} are small in comparison to c_{ii} and d_{ii}. Hence the i^{th} mode shape of the uniform system may be regarded as a first approximation to the i^{th} mode shape of the non-uniform system.

The form of the governing equation, equation (85), "has the advantage that any of the higher frequencies and mode shapes may be calculated directly, without first calculating the lower mode shapes."[7]

To determine any mode shape ϕ_r and the corresponding natural frequency ω_r, b_r is taken equal to one and a first approximation for ϕ_r and ω_r is obtained by neglecting the products of small quantities. Successive approximations are obtained by considering an increasing number of equations and the previously neglected small quantities.

"This iteration method, though based on the assumption of small differences between the non-uniform and uniform systems, may often be used successfully in cases where the mass and inertia distributions of the two systems differ considerably."[7]

PROBLEMS CONSIDERED

The problems specifically considered in this thesis are simply-supported beams of constant width and depths which vary lineary and parabolically along the length of the beam.

Due to the depth variations, the area and moment of inertia functions, $\rho(x)$ and $\psi(x)$, were of such form, that the differential equation of motion, equation (5), was virtually impossible to solve exactly.

Because of the impossibility of solving the differential equation of motion exactly, the Rayleigh-Ritz method and the Jones technique[7] were used to generate the low order natural frequencies and the series expansion coefficients which defined the corresponding mode shapes.

The equations used to calculate the low order frequencies and mode shapes were:

$$\omega_i^2 \sum_{K=1}^{\infty} c_{IK} b_K^i - \sum_{K=1}^{\infty} d_{IK} b_K^i = 0 \qquad (85)$$

$$i = 1, 2, 3, \ldots \infty$$

and

$$\phi_i = \sum_{k=1}^{\infty} b_k^i \bar{\phi}_k \tag{86}$$

$$i = 1,\ 2,\ 3,\ \ldots \infty$$

where

$$c_{IK} = \int_0^1 m \bar{\phi}_I \bar{\phi}_K dx \quad \text{and} \tag{83}$$

$$d_{IK} = \int_0^1 EI \bar{\phi}_I'' \bar{\phi}_K'' dx \tag{84}$$

The $\bar{\phi}$ functions for a simply-supported beam are $\sin n\pi\eta$ - see derivation of equation (61). Due to the variation in m and I, the general formulas for coefficients c_{IK} and d_{IK} were extremely complicated - see Appendix B - and as a result, equations (85) could not be solved in general terms.

Solutions were obtained for simply-supported beams symmetrically haunched about the beam centerline and with specifically assigned depth ratios (τ) of 1.0, 1.4, 1.8, 2.2, 2.6, and 3.0 (Figs. 3a and 3b).

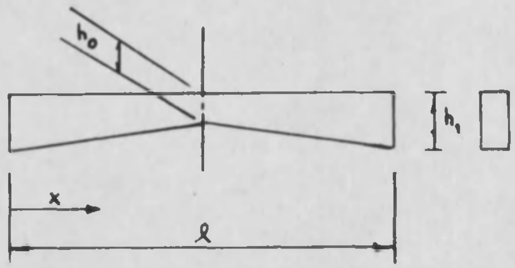

Depth Ratio $T = h_1 / h_o$

Linear Taper - Symmetric Beam

Fig. 3a

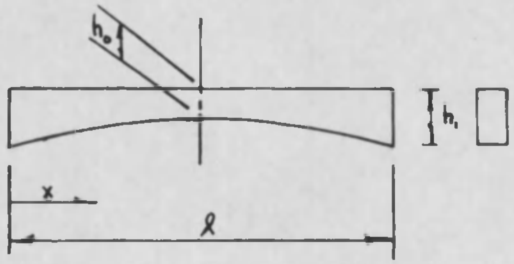

Depth Ratio $T = h_1 / h_o$

Parabolic Taper - Symmetric Beam

Fig. 3b

It was found - see Appendix C for derivation - that the results generated for the symmetric beams could be used for certain simply-supported unsymmetric beams (Figs. 4a and 4b).

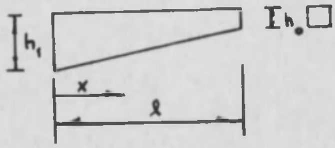

Depth Ratio $\tau = h_1 / h_0$

Linear Taper - Unsymmetric Beam

Fig. 4a

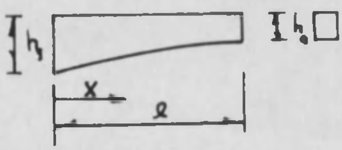

Depth Ratio $\tau = h_1 / h_0$

Parabolic Taper - Unsymmetric Beam

Fig. 4b

RESULTS

With the beam configurations and depth ratios thus specified, the evaluation of the c_{IK} and d_{IK} coefficients and the iterative solution of the simultaneous equations (85) were programmed for and calculated by an IBM 7072 computer.

The computer was programmed to solve the first twenty equations of equations (85). The computer results are given in graphical and tabular form as follows:

The frequency ratio - depth ratio curves (Figs. 5-8) indicate the variation of the low order frequencies (first six for the symmetric beams and first three for the unsymmetric beams) as the depth ratio is changed. The frequency ratios become practically identical at frequencies higher than the second natural frequency as evidenced by the grouping of the curves. For depth ratios between one and three and for beams of the configuration shown, Figures 5-8 may be used to calculate the low order natural frequencies of a non-uniform beam by using the appropriate numerical value of the frequency ratio and multiplying by the corresponding natural frequency for a simply-supported

FREQUENCY RATIO - DEPTH RATIO

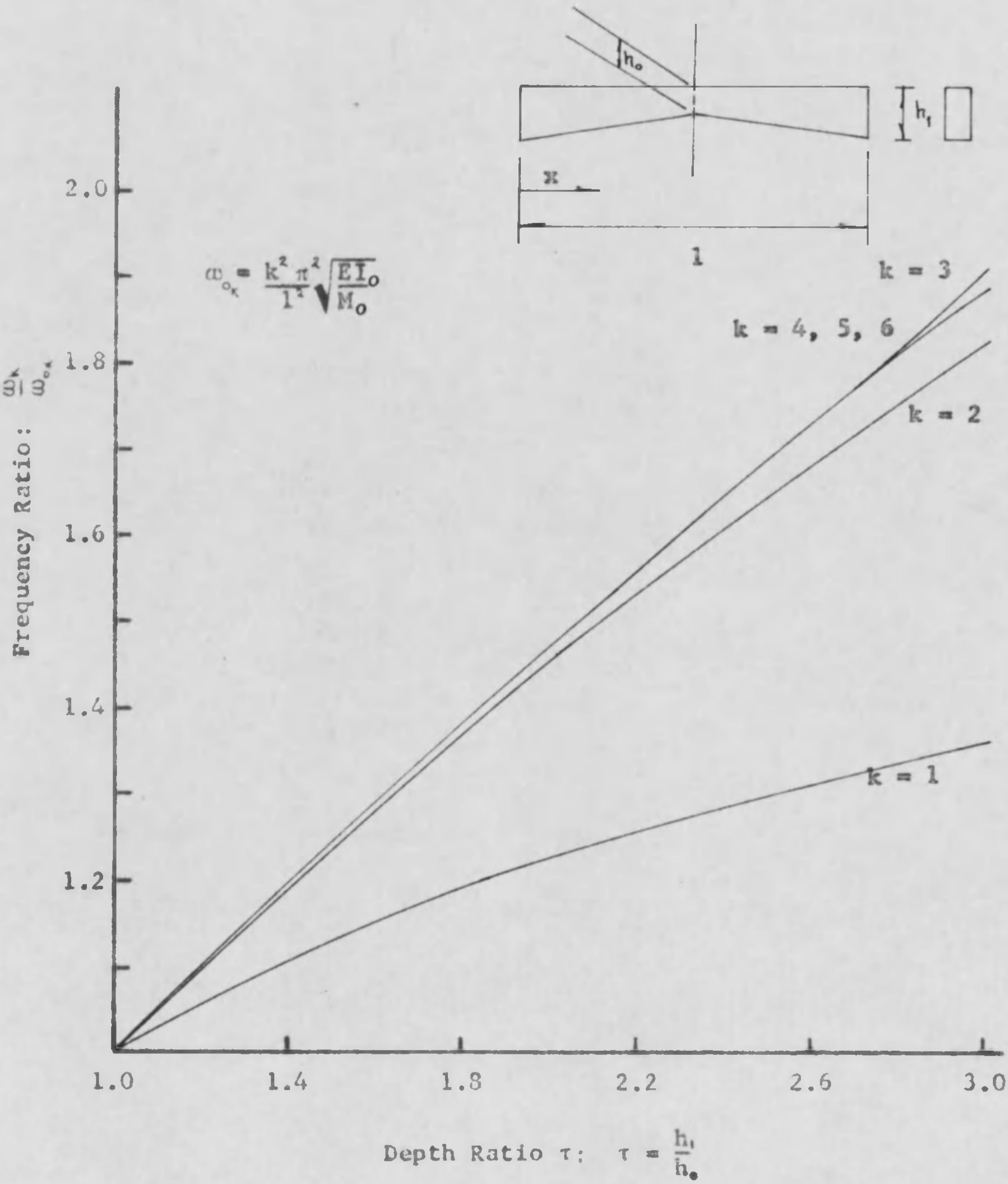

Fig. 5

Linear Taper - Symmetric Beam

FREQUENCY RATIO - DEPTH RATIO

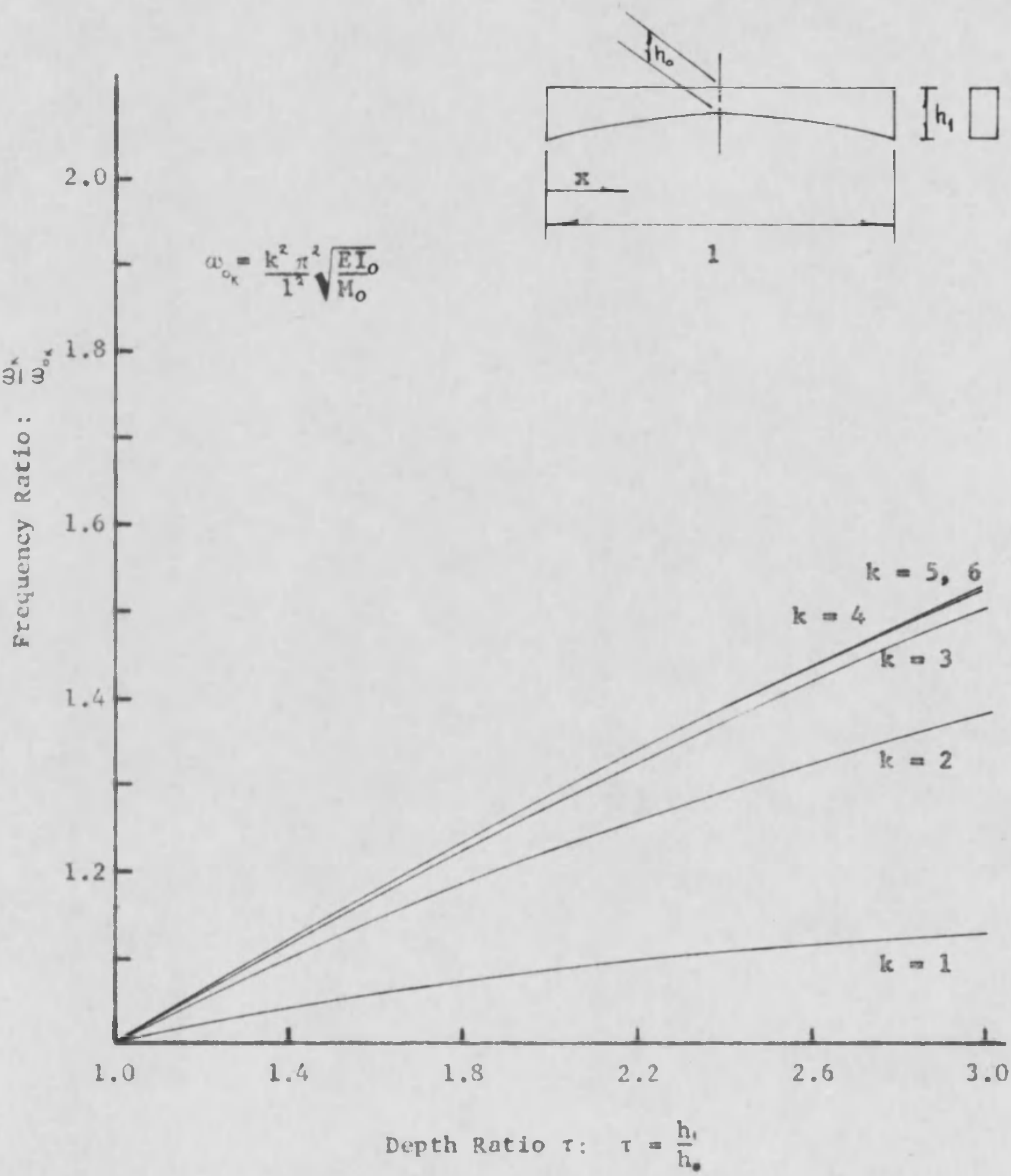

Fig. 6

Parabolic Taper - Symmetric Beam

FREQUENCY RATIO - DEPTH RATIO

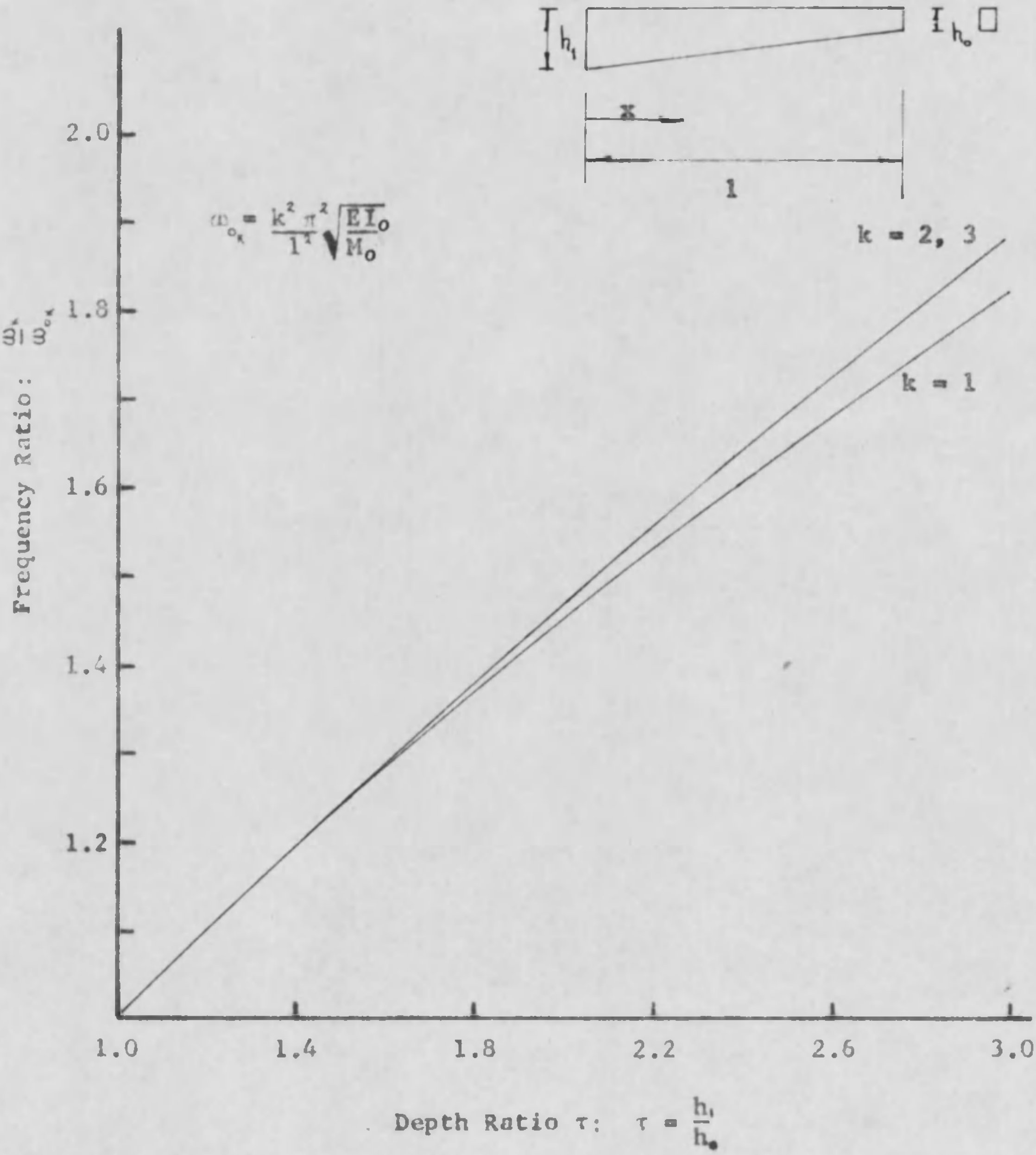

Fig. 7

Linear Taper - Unsymmetric Beam

FREQUENCY RATIO - DEPTH RATIO

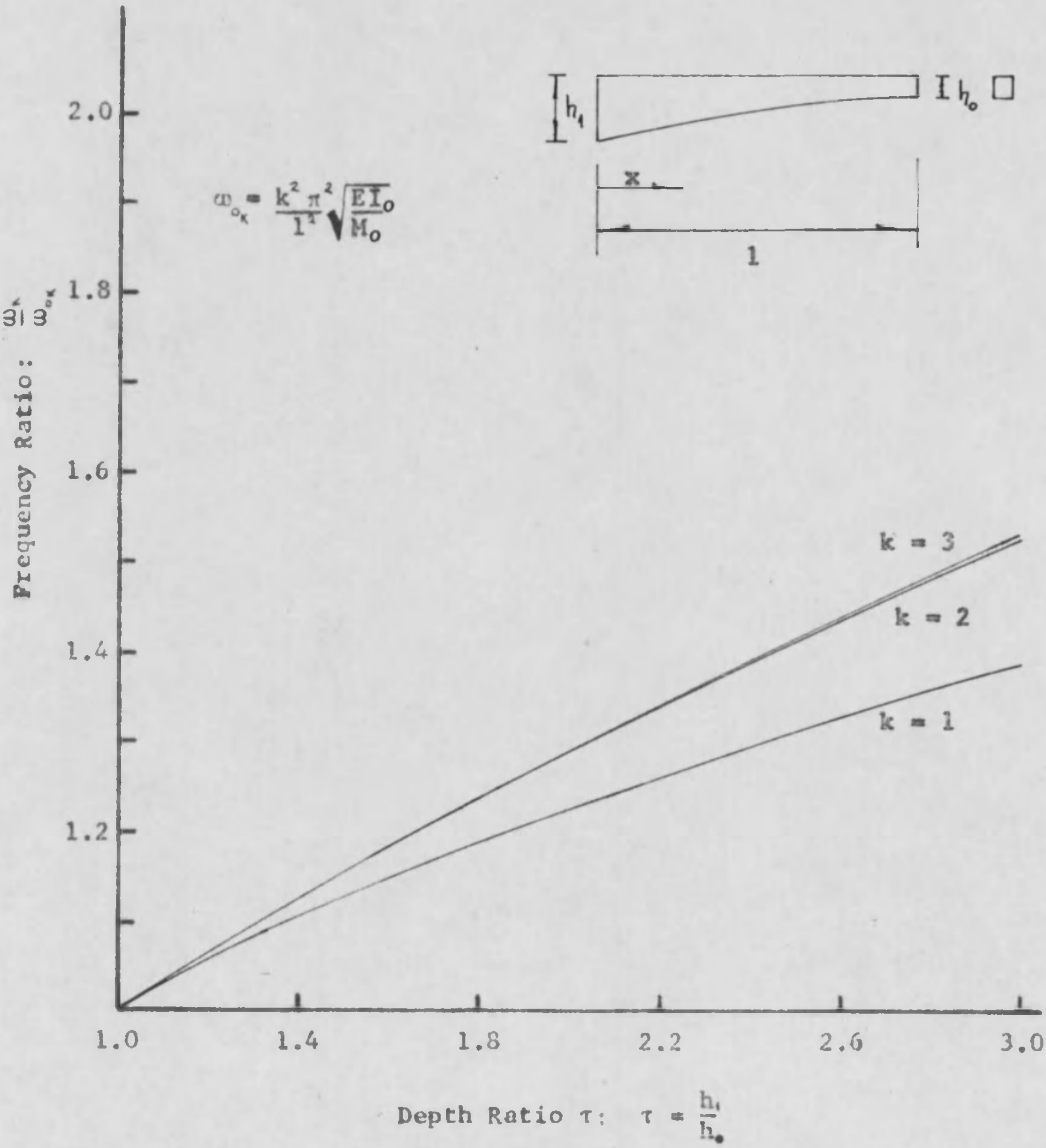

Fig. 8

Parabolic Taper - Unsymmetric Beam

uniform beam of depth h_o.

Tables 1-10 are tabulations of the b_K^i coefficients of series (86) which defines the mode shapes of the non-uniform beam. The coefficients are tabulated for the first six mode shapes for the symmetric beams. The coefficients for the first three mode shapes of the unsymmetric beams are calculated from Tables 1-10 by using the second, fourth, and sixth mode shape values for the symmetric beam, half of which is the particular unsymmetric beam. The tabulated coefficients verify Jones'[7] theory that the resulting coefficients are smaller than the particular coefficient chosen to be unity, ie., the r^{th} mode shape of the uniform beam is a good first approximation for the r^{th} mode shape of the non-uniform beam.

Figures 9-16 show graphical representations of the first three mode shapes for all the considered beams for depth ratios of 2.2 and 3.0.

Tables 11-18 are listings of the values used to plot Figs. 9-16. The values in Tables 11-18 were found by summing the first twenty terms of series (86).

Figures 17-20 indicate the distortion of the first mode shape for all four beams studied as compared to the

TABLES 1 - 10

I. General notes.

1. The Series Expansion Coefficients are for the series

$$\phi_i = \sum_{j=1}^{20} b_j^i \sin j\pi\eta$$

$$i = 1, 2, 3, 4, 5, 6.$$

2. All the even coefficients(b_2, b_4, ...) are zero for the odd mode shapes($i = 1, 3, 5$).

3. All the odd coefficients(b_1, b_3, ...) are zero for the even mode shapes($i = 2, 4, 6$).

4. Interpretation of table values:

$$-3.60789\text{E-}02 = -3.60789 \times 10^{-2}$$

Table 1

SERIES EXPANSION COEFFICIENTS

Linear Taper - Symmetric Beam - Depth Ratio $\tau = 1.4$

Odd Modes	Even Modes	First Mode $i = 1$	Second Mode $i = 2$	Third Mode $i = 3$	Fourth Mode $i = 4$	Fifth Mode $i = 5$	Sixth Mode $i = 6$
b_1	b_2	1.00000E 00	1.00000E 00	-5.06351E-02	-1.60111E-02	8.24471E-03	2.93781E-04
b_3	b_4	-2.12806E-02	-4.43028E-02	1.00000E 00	1.00000E 00	4.79722E-03	2.72103E-02
b_5	b_6	1.97054E-03	2.75292E-03	-7.37376E-02	-9.22762E-02	1.00000E 00	1.00000E 00
b_7	b_8	-6.02056E-04	-1.08067E-03	6.86287E-03	7.59110E-03	-1.16456E-01	-1.33588E-01
b_9	b_{10}	1.90845E-04	1.97969E-04	-3.02538E-03	-3.47796E-03	1.20314E-02	1.34028E-02
b_{11}	b_{12}	-9.45717E-05	-1.36429E-04	8.40601E-04	6.88132E-04	-5.65567E-03	-6.13828E-03
b_{13}	b_{14}	4.40620E-05	3.59873E-05	-5.52704E-04	-5.46595E-04	1.49761E-03	1.32270E-03
b_{15}	b_{16}	-2.65009E-05	-3.17306E-05	2.23773E-04	1.43635E-04	-1.11247E-03	-1.08171E-03
b_{17}	b_{18}	1.47077E-05	9.86215E-06	-1.67096E-04	-1.43551E-04	4.14029E-04	2.95745E-04
b_{19}	b_{20}	-8.66167E-06	-9.50083E-06	6.86487E-05	3.23726E-05	-3.24660E-04	-2.92951E-04

Table 2

SERIES EXPANSION COEFFICIENTS

Linear Taper - Symmetric Beam - Depth Ratio $\tau = 1.8$

Odd Modes	Even Modes	First Mode $i = 1$	Second Mode $i = 2$	Third Mode $i = 3$	Fourth Mode $i = 4$	Fifth Mode $i = 5$	Sixth Mode $i = 6$
b_1	b_2	1.00000E 00	1.00000E 00	-9.41569E-02	-2.74406E-02	1.68144E-02	8.86653E-04
b_3	b_4	-3.58246E-02	-7.68860E-02	1.00000E 00	1.00000E 00	5.99982E-03	4.76065E-02
b_5	b_6	4.63601E-03	8.28722E-03	-1.27102E-01	-1.59894E-01	1.00000E 00	1.00000E 00
b_7	b_8	-1.34813E-03	-2.53696E-03	1.86005E-02	2.27963E-02	-2.01531E-01	-2.32014E-01
b_9	b_{10}	4.76081E-04	6.78377E-04	-6.81268E-03	-8.12719E-03	3.44135E-02	4.03644E-02
b_{11}	b_{12}	-2.23328E-04	-3.39081E-04	2.33285E-03	2.35060E-03	-1.31873E-02	-1.48840E-02
b_{13}	b_{14}	1.10322E-04	1.27399E-04	-1.28601E-03	-1.31744E-03	4.50409E-03	4.60033E-03
b_{15}	b_{16}	-6.28508E-05	-7.95585E-05	5.99708E-04	4.99764E-04	-2.61371E-03	-2.64208E-03
b_{17}	b_{18}	3.54692E-05	3.44165E-05	-3.79767E-04	-3.37937E-04	1.16531E-03	1.02202E-03
b_{19}	b_{20}	-1.81813E-05	-2.11400E-05	1.60456E-04	1.07899E-04	-6.76429E-04	-6.34124E-04

Table 3

SERIES EXPANSION COEFFICIENTS

Linear Taper - Symmetric Beam - Depth Ratio $\mathcal{T} = 2.2$

Odd Modes	Even Modes	First Mode i = 1	Second Mode i = 2	Third Mode i = 3	Fourth Mode i = 4	Fifth Mode i = 5	Sixth Mode i = 6
b_1	b_2	1.00000E 00	1.00000E 00	-1.31929E-01	-3.59945E-02	2.54576E-02	1.57462E-03
b_3	b_4	-4.64658E-02	-1.02337E-01	1.00000E 00	1.00000E 00	5.05428E-03	6.39656E-02
b_5	b_6	7.29988E-03	1.46732E-02	-1.68029E-01	-2.12439E-01	1.00000E 00	1.00000E 00
b_7	b_8	-2.17939E-03	-4.39048E-03	3.14690E-02	4.02472E-02	-2.67379E-01	-3.09074E-01
b_9	b_{10}	8.15363E-04	1.36859E-03	-1.12806E-02	-1.39984E-02	5.95974E-02	7.14887E-02
b_{11}	b_{12}	-3.80298E-04	-6.30508E-04	4.24763E-03	4.72242E-03	-2.24971E-02	-2.62774E-02
b_{13}	b_{14}	1.92362E-04	2.67736E-04	-2.21068E-03	-2.39268E-03	8.56804E-03	9.38748E-03
b_{15}	b_{16}	-1.07414E-04	-1.50327E-04	1.08586E-03	1.03109E-03	-4.57023E-03	-4.85259E-03
b_{17}	b_{18}	6.00421E-05	7.14959E-05	-6.37023E-04	-6.05187E-04	2.15344E-03	2.09338E-03
b_{19}	b_{20}	-2.82958E-05	-3.62912E-05	2.65235E-04	2.13513E-04	-1.07333E-03	-1.06033E-03

Table 4

SERIES EXPANSION COEFFICIENTS

Linear Taper - Symmetric Beam - Depth Ratio $\tau = 2.6$

Odd Modes	Even Modes	First Mode $i = 1$	Second Mode $i = 2$	Third Mode $i = 3$	Fourth Mode $i = 4$	Fifth Mode $i = 5$	Sixth Mode $i = 6$
b_1	b_2	1.00000E 00	1.00000E 00	-1.65018E-01	-4.26197E-02	3.40454E-02	2.28194E-03
b_3	b_4	-5.46066E-02	-1.23014E-01	1.00000E 00	1.00000E 00	2.70455E-03	7.76293E-02
b_5	b_6	9.76290E-03	2.11873E-02	-2.00633E-01	-2.54884E-01	1.00000E 00	1.00000E 00
b_7	b_8	-3.03196E-03	-6.51679E-03	4.41293E-02	5.79393E-02	-3.20271E-01	-3.71802E-01
b_9	b_{10}	1.18210E-03	2.22099E-03	-1.61173E-02	-2.06819E-02	8.47755E-02	1.03228E-01
b_{11}	b_{12}	-5.55687E-04	-1.00588E-03	6.43502E-03	7.62724E-03	-3.28769E-02	-3.94554E-02
b_{13}	b_{14}	2.85053E-04	4.53403E-04	-3.28541E-03	-3.74961E-03	1.33668E-02	1.53432E-02
b_{15}	b_{16}	-1.57671E-04	-2.44546E-04	1.65317E-03	1.71557E-03	-6.90292E-03	-7.66556E-03
b_{17}	b_{18}	8.68968E-05	1.20144E-04	-9.28135E-04	-9.42692E-04	3.31577E-03	3.45785E-03
b_{19}	b_{20}	-3.86424E-05	-5.49859E-05	3.77542E-04	3.42822E-04	-1.50754E-03	-1.56826E-03

Table 5

SERIES EXPANSION COEFFICIENTS

Linear Taper - Symmetric Beam - Depth Ratio $\mathcal{T}$ = 3.0

Odd Modes	Even Modes	First Mode $i = 1$	Second Mode $i = 2$	Third Mode $i = 3$	Fourth Mode $i = 4$	Fifth Mode $i = 5$	Sixth Mode $i = 6$
b_1	b_2	1.00000E 00	1.00000E 00	-1.94257E-01	-4.78887E-02	4.25067E-02	2.97697E-03
b_3	b_4	-6.10362E-02	-1.40288E-01	1.00000E 00	1.00000E 00	-6.15867E-04	8.93553E-02
b_5	b_6	1.19790E-02	2.75359E-02	-2.27318E-01	-2.90131E-01	1.00000E 00	1.00000E 00
b_7	b_8	-3.86666E-03	-8.80461E-03	5.60834E-02	7.50683E-02	-3.63862E-01	-4.24265E-01
b_9	b_{10}	1.55787E-03	3.19395E-03	-2.10767E-02	-2.78146E-02	1.08827E-01	1.34108E-01
b_{11}	b_{12}	-7.40976E-04	-1.45296E-03	8.77858E-03	1.09117E-02	-4.37315E-02	-5.36474E-02
b_{13}	b_{14}	3.84064E-04	6.79322E-04	-4.46236E-03	-5.33786E-03	1.86244E-02	2.21402E-02
b_{15}	b_{16}	-2.11330E-04	-3.60459E-04	2.27583E-03	2.52791E-03	-9.50312E-03	-1.09677E-02
b_{17}	b_{18}	1.14867E-04	1.79158E-04	-1.24157E-03	-1.34037E-03	4.59653E-03	5.05758E-03
b_{19}	b_{20}	-4.89238E-05	-7.68557E-05	4.93395E-04	4.90560E-04	-1.96562E-03	-2.14262E-03

Table 6

SERIES EXPANSION COEFFICIENTS

Parabolic Taper - Symmetric Beam - Depth Ratio $\tau = 1.4$

Odd Modes	Even Modes	First Mode i = 1	Second Mode i = 2	Third Mode i = 3	Fourth Mode i = 4	Fifth Mode i = 5	Sixth Mode i = 6
b_1	b_2	1.00000E 00	1.00000E 00	-3.98207E-02	-1.81896E-02	-9.02689E-03	-9.02867E-03
b_3	b_4	-1.61894E-02	-4.49969E-02	1.00000E 00	1.00000E 00	5.91093E-03	2.84601E-02
b_5	b_6	-3.15838E-04	-1.43532E-03	-7.14725E-02	-9.52596E-02	1.00000E 00	1.00000E 00
b_7	b_8	-7.35773E-05	-3.82882E-04	-2.64051E-03	-3.50243E-03	-1.17435E-01	-1.38659E-01
b_9	b_{10}	-2.04980E-05	-1.19585E-04	-8.34545E-04	-1.31825E-03	-3.92355E-03	-3.89625E-03
b_{11}	b_{12}	-7.46576E-06	-4.71030E-05	-2.84201E-04	-4.79279E-04	-1.78652E-03	-2.22121E-03
b_{13}	b_{14}	-3.23059E-06	-2.15016E-05	-1.18958E-04	-2.10884E-04	-6.83671E-04	-8.83147E-04
b_{15}	b_{16}	-1.58284E-06	-1.09943E-05	-5.71235E-05	-1.05213E-04	-3.14424E-04	-4.20507E-04
b_{17}	b_{18}	-8.58175E-07	-6.15940E-06	-3.05356E-05	-5.79725E-05	-1.63411E-04	-2.24646E-04
b_{19}	b_{20}	-5.83339E-07	-4.31633E-06	-2.05797E-05	-4.01107E-05	-1.07902E-04	-1.51980E-04

Table 7

SERIES EXPANSION COEFFICIENTS

Parabolic Taper - Symmetric Beam - Depth Ratio $\mathcal{T} = 1.8$

Odd Modes	Even Modes	First Mode $i = 1$	Second Mode $i = 2$	Third Mode $i = 3$	Fourth Mode $i = 4$	Fifth Mode $i = 5$	Sixth Mode $i = 6$
b_1	b_2	1.00000E 00	1.00000E 00	-7.70116E-02	-3.43121E-02	-1.66776E-02	-1.63466E-02
b_3	b_4	-2.76052E-02	-7.90381E-02	1.00000E 00	1.00000E 00	1.05420E-02	5.17269E-02
b_5	b_6	4.47486E-04	1.21005E-03	-1.26574E-01	-1.69195E-01	1.00000E 00	1.00000E 00
b_7	b_8	-7.59317E-05	-4.18786E-04	2.47153E-03	4.73144E-03	-2.09253E-01	-2.48060E-01
b_9	b_{10}	-1.53893E-05	-1.04653E-04	-9.67294E-04	-1.61804E-03	8.17399E-03	1.28595E-02
b_{11}	b_{12}	-5.96802E-06	-4.30027E-05	-2.62606E-04	-4.50225E-04	-2.34248E-03	-3.14535E-03
b_{13}	b_{14}	-2.60636E-06	-1.98245E-05	-1.14997E-04	-2.08916E-04	-6.43357E-04	-8.23662E-04
b_{15}	b_{16}	-1.28544E-06	-1.02080E-05	-5.56887E-05	-1.05135E-04	-3.16684E-04	-4.28199E-04
b_{17}	b_{18}	-6.90081E-07	-5.64725E-06	-2.94607E-05	-5.73399E-05	-1.63158E-04	-2.26661E-04
b_{19}	b_{20}	-5.52957E-07	-4.66777E-06	-2.33692E-05	-4.68173E-05	-1.27078E-04	-1.81556E-04

Table 8

SERIES EXPANSION COEFFICIENTS

Parabolic Taper - Symmetric Beam - Depth Ratio $T = 2.2$

Odd Modes	Even Modes	First Mode $i = 1$	Second Mode $i = 2$	Third Mode $i = 3$	Fourth Mode $i = 4$	Fifth Mode $i = 5$	Sixth Mode $i = 6$
b_1	b_2	1.00000E 00	1.00000E 00	-1.11595E-01	-4.85950E-02	-2.33640E-02	-2.26072E-02
b_3	b_4	-3.62209E-02	-1.06239E-01	1.00000E 00	1.00000E 00	1.45167E-02	7.18741E-02
b_5	b_6	1.60371E-03	5.67405E-03	-1.71200E-01	-2.29365E-01	1.00000E 00	1.00000E 00
b_7	b_8	-1.34187E-04	-6.72517E-04	1.12098E-02	1.85349E-02	-2.84565E-01	-3.38783E-01
b_9	b_{10}	-5.97701E-06	-6.05610E-05	-1.56700E-03	-2.76185E-03	2.79992E-02	3.98020E-02
b_{11}	b_{12}	-4.56657E-06	-3.60577E-05	-1.63160E-04	-2.71994E-04	-4.29659E-03	-6.24605E-03
b_{13}	b_{14}	-1.87568E-06	-1.60247E-05	-1.00720E-04	-1.87908E-04	-3.55168E-04	-3.82481E-04
b_{15}	b_{16}	-9.43095E-07	-8.37961E-06	-4.73307E-05	-9.12150E-05	-2.93131E-04	-4.07839E-04
b_{17}	b_{18}	-4.87079E-07	-4.45202E-06	-2.42716E-05	-4.82040E-05	-1.37620E-04	-1.92834E-04
b_{19}	b_{20}	-4.56607E-07	-4.31365E-06	-2.24979E-05	-4.61212E-05	-1.26490E-04	-1.83468E-04

Table 9

SERIES EXPANSION COEFFICIENTS

Parabolic Taper - Symmetric Beam - Depth Ratio $\tau = 2.6$

Odd Modes	Even Modes	First Mode $i = 1$	Second Mode $i = 2$	Third Mode $i = 3$	Fourth Mode $i = 4$	Fifth Mode $i = 5$	Sixth Mode $i = 6$
b_1	b_2	1.00000E 00	1.00000E 00	-1.43751E-01	-6.13269E-02	-2.93340E-02	-2.81511E-02
b_3	b_4	-4.30197E-02	-1.28764E-01	1.00000E 00	1.00000E 00	1.80927E-02	8.99249E-02
b_5	b_6	2.88939E-03	1.09717E-02	-2.08530E-01	-2.79889E-01	1.00000E 00	1.00000E 00
b_7	b_8	-2.60603E-04	-1.24695E-03	2.17048E-02	3.50778E-02	-3.48312E-01	-4.16502E-01
b_9	b_{10}	1.06365E-05	2.31485E-05	-2.86806E-03	-5.12052E-03	5.17286E-02	7.21103E-02
b_{11}	b_{12}	-4.60721E-06	-3.54907E-05	3.69810E-05	1.04313E-04	-8.16470E-03	-1.22029E-02
b_{13}	b_{14}	-1.25973E-06	-1.23173E-05	-1.00878E-04	-1.94522E-04	2.81904E-04	6.31257E-04
b_{15}	b_{16}	-7.07044E-07	-6.89052E-06	-3.83993E-05	-7.51065E-05	-3.20197E-04	-4.74167E-04
b_{17}	b_{18}	-3.38576E-07	-3.40326E-06	-1.94603E-05	-3.93263E-05	-1.05851E-04	-1.46958E-04
b_{19}	b_{20}	-3.70753E-07	-3.86353E-06	-2.08662E-05	-4.36227E-05	-1.21565E-04	-1.79211E-04

Table 10

SERIES EXPANSION COEFFICIENTS

Parabolic Taper - Symmetric Beam - Depth Ratio τ = 3.0

Odd Modes	Even Modes	First Mode i = 1	Second Mode i = 2	Third Mode i = 3	Fourth Mode i = 4	Fifth Mode i = 5	Sixth Mode i = 6
b_1	b_2	1.00000E 00	1.00000E 00	-1.73685E-01	-7.27607E-02	-3.47479E-02	-3.31783E-02
b_3	b_4	-4.85565E-02	-1.47890E-01	1.00000E 00	1.00000E 00	2.13897E-02	1.06460E-01
b_5	b_6	4.19177E-03	1.66210E-02	-2.40482E-01	-3.23273E-01	1.00000E 00	1.00000E 00
b_7	b_8	-4.43783E-04	-2.12309E-03	3.30123E-02	5.29131E-02	-4.03503E-01	-4.84634E-01
b_9	b_{10}	3.77053E-05	1.64788E-04	-4.84502E-03	-8.64453E-03	7.73979E-02	1.07289E-01
b_{11}	b_{12}	-6.85269E-06	-4.67585E-05	3.80644E-04	7.56296E-04	-1.38651E-02	-2.09071E-02
b_{13}	b_{14}	-5.62587E-07	-7.93653E-06	-1.30462E-04	-2.59041E-04	1.39836E-03	2.43095E-03
b_{15}	b_{16}	-5.77910E-07	-5.95854E-06	-2.72527E-05	-5.34076E-05	-4.51348E-04	-7.16896E-04
b_{17}	b_{18}	-2.33815E-07	-2.56838E-06	-1.60410E-05	-3.29680E-05	-6.20586E-05	-7.69522E-05
b_{19}	b_{20}	-3.03558E-07	-3.44841E-06	-1.91463E-05	-4.07144E-05	-1.17723E-04	-1.77131E-04

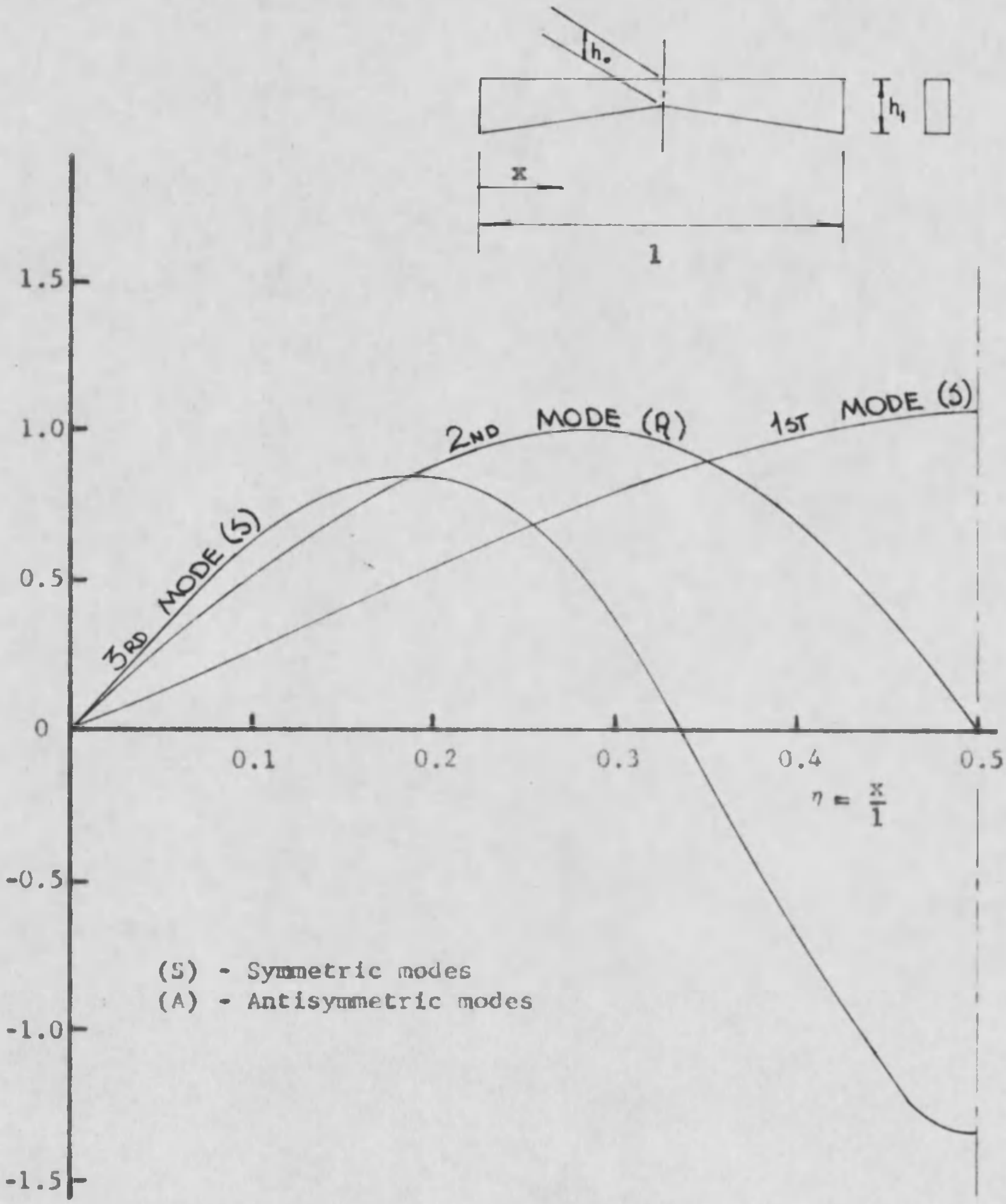

Fig. 9

FIRST THREE MODE SHAPES

Linear Taper - Symmetric Beam - Depth Ratio $\tau = 2.2$

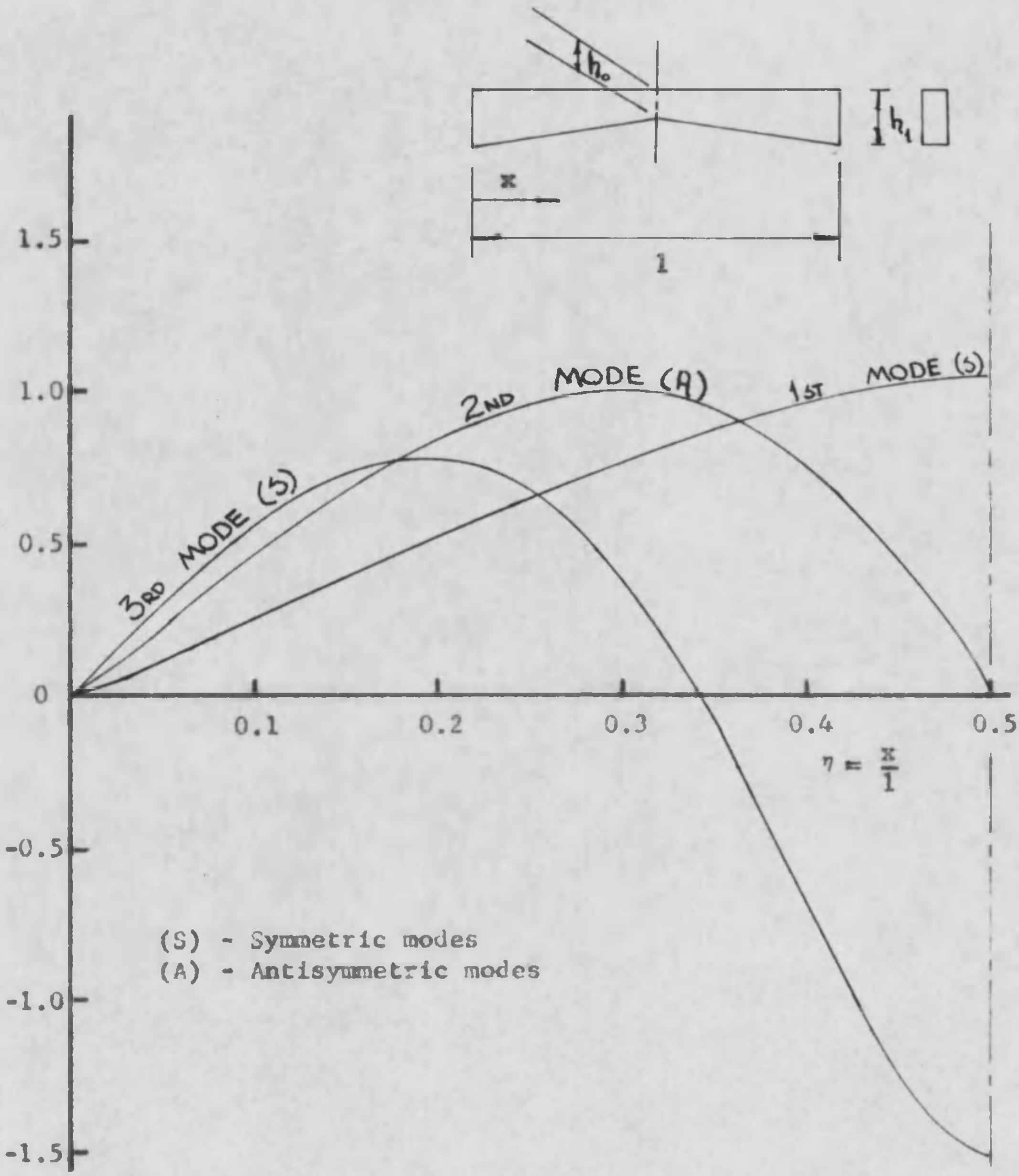

Fig. 10

FIRST THREE MODE SHAPES

Linear Taper - Symmetric Beam - Depth Ratio $\tau = 3.0$

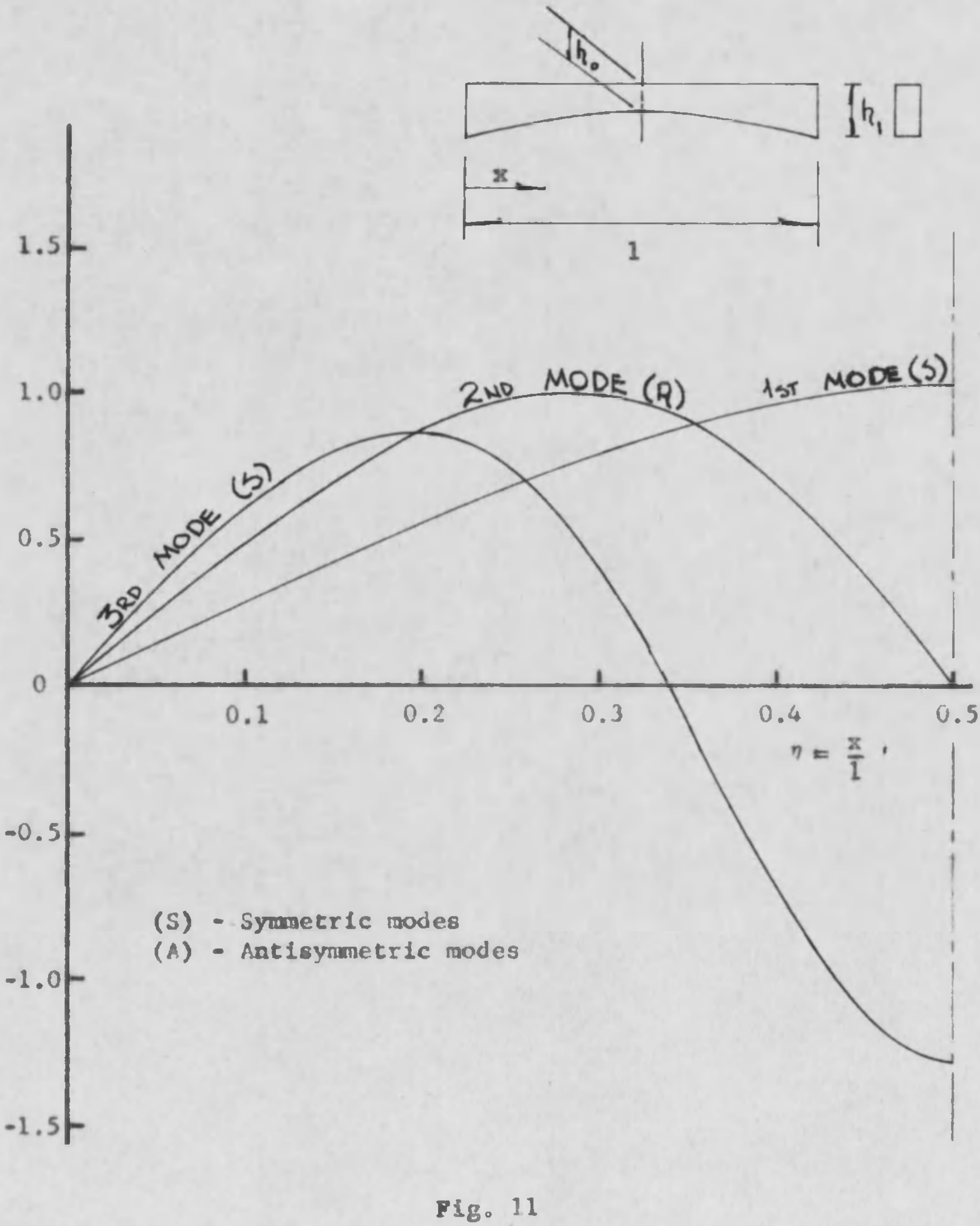

Fig. 11

FIRST THREE MODE SHAPES

Parabolic Taper - Symmetric Beam - Depth Ratio $\tau = 2.2$

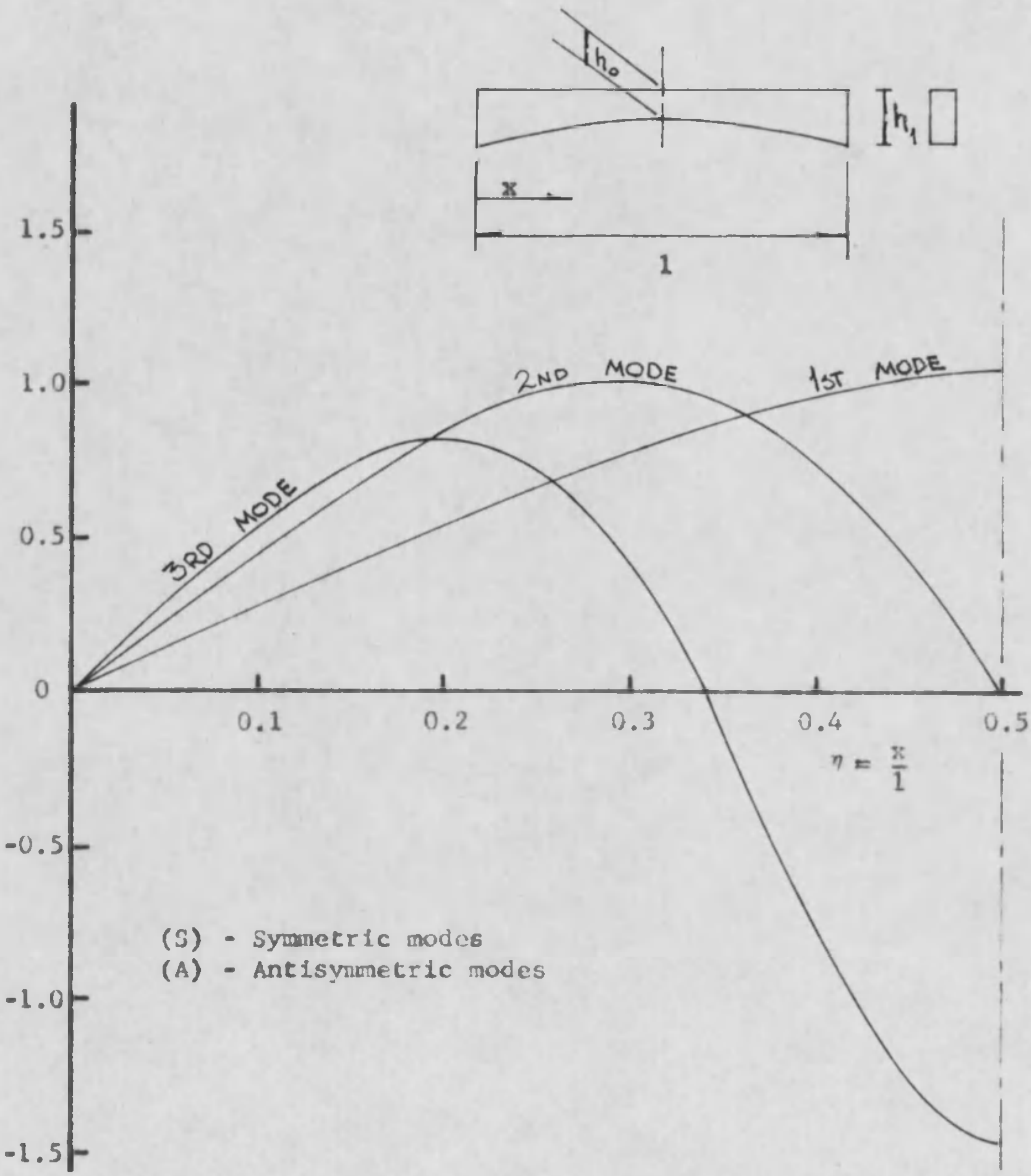

Fig. 12

FIRST THREE MODE SHAPES

Parabolic Taper - Symmetric Beam - Depth Ratio $\tau = 3.0$

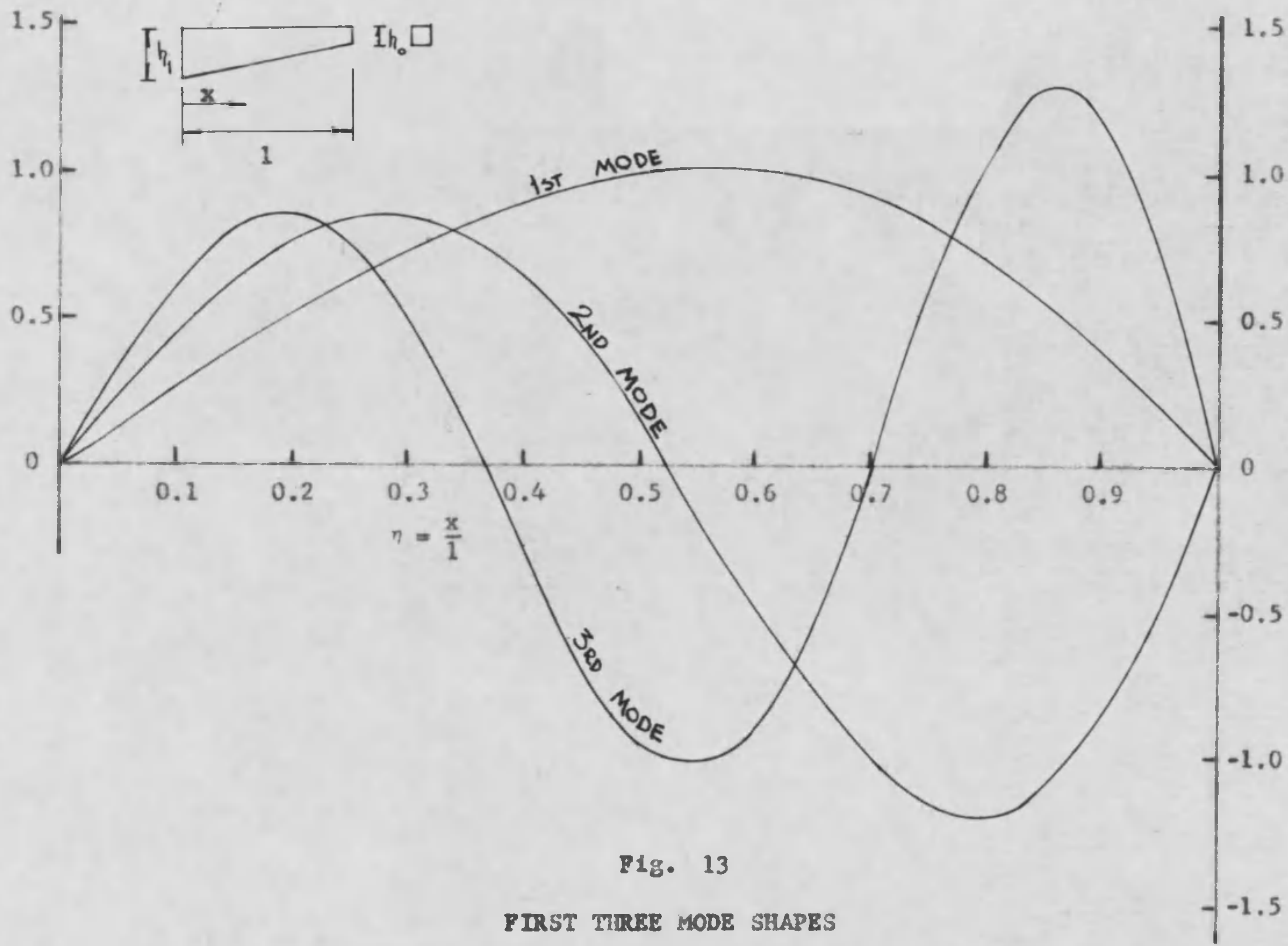

Fig. 13

FIRST THREE MODE SHAPES

Linear Taper - Unsymmetric Beam - Depth Ratio $\tau = 2.2$

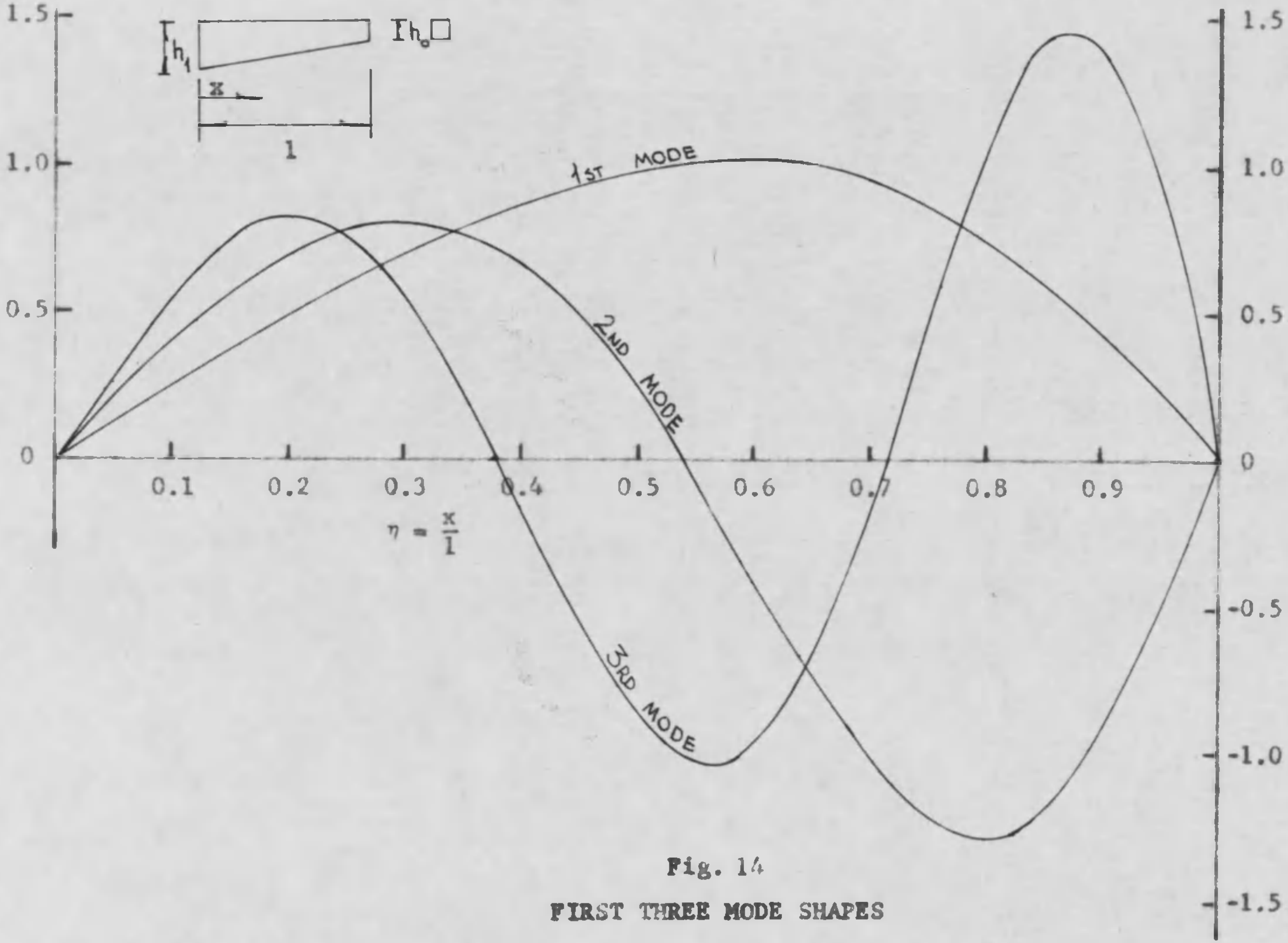

Fig. 14

FIRST THREE MODE SHAPES

Linear Taper - Unsymmetric Beam - Depth Ratio τ = 3.0

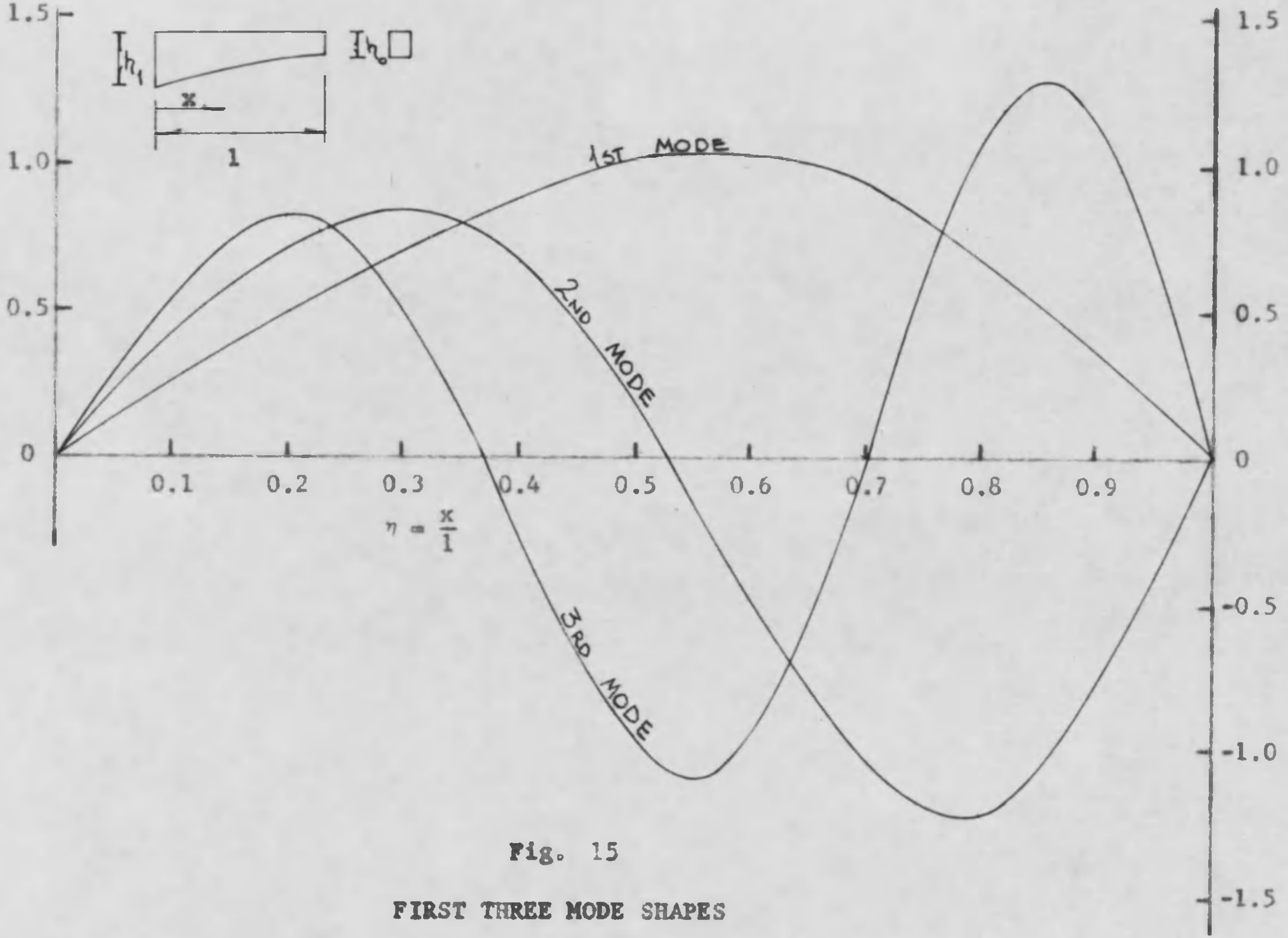

Fig. 15

FIRST THREE MODE SHAPES

Parabolic Taper - Unsymmetric Beam - Depth Ratio $\tau = 2.2$

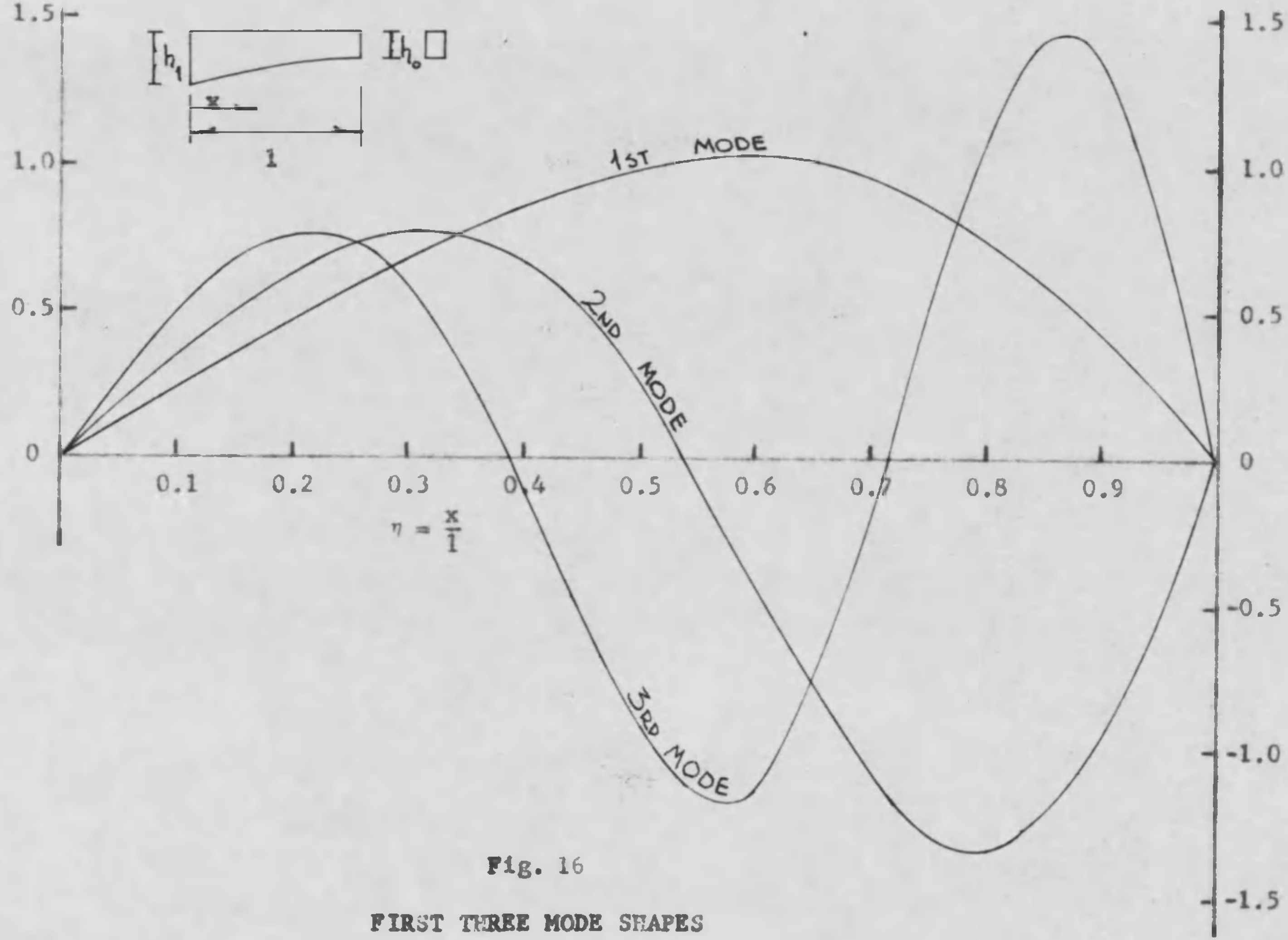

Fig. 16

FIRST THREE MODE SHAPES

Parabolic Taper - Unsymmetric Beam - Depth Ratio τ = 3.0

Table 11

MODE SHAPE ORDINATES -- FIRST THREE MODES

Linear Taper - Symmetric Beam - Depth Ratio τ = 2.2

$\eta = \frac{x}{l}$	First Mode Shape Ordinate	Second Mode Shape Ordinate	Third Mode Shape Ordinate
0.00	0.0000	0.0000	0.0000
0.04	0.1113	0.2066	0.2695
0.08	0.2222	0.4067	0.5157
0.12	0.3320	0.5928	0.7125
0.16	0.4399	0.7559	0.8323
0.20	0.5451	0.8860	0.8511
0.24	0.6464	0.9728	0.7507
0.28	0.7422	1.0057	0.5256
0.32	0.8307	0.9755	0.1872
0.36	0.9097	0.8748	-0.2337
0.40	0.9759	0.7008	-0.6793
0.44	1.0257	0.4577	-1.0734
0.48	1.0538	0.1600	-1.3176
0.52	1.0538	-0.1600	-1.3176
0.56	1.0257	-0.4577	-1.0734
0.60	0.9759	-0.7008	-0.6793
0.64	0.9097	-0.8748	-0.2337
0.68	0.8307	-0.9755	0.1872
0.72	0.7422	-1.0057	0.5256
0.76	0.6464	-0.9728	0.7507
0.80	0.5451	-0.8860	0.8511
0.84	0.4399	-0.7559	0.8323
0.88	0.3320	-0.5928	0.7125
0.92	0.2222	-0.4067	0.5157
0.96	0.1113	-0.2066	0.2695
1.00	0.0000	0.0000	0.0000

Table 12

MODE SHAPE ORDINATES -- FIRST THREE MODES

Linear Taper - Symmetric Beam - Depth Ratio τ = 3.0

$\eta = \frac{x}{l}$	First Mode Shape Ordinate	Second Mode Shape Ordinate	Third Mode Shape Ordinate
0.00	0.0000	0.0000	0.0000
0.04	0.1079	0.1945	0.2399
0.08	0.2155	0.3844	0.4620
0.12	0.3224	0.5637	0.6452
0.16	0.4283	0.7252	0.7649
0.20	0.5323	0.8598	0.7977
0.24	0.6339	0.9578	0.7212
0.28	0.7316	1.0074	0.5221
0.32	0.8239	0.9969	0.1999
0.36	0.9087	0.9145	-0.2277
0.40	0.9824	0.7506	-0.7097
0.44	1.0406	0.5023	-1.1685
0.48	1.0752	0.1785	-1.4728
0.52	1.0752	-0.1785	-1.4728
0.56	1.0406	-0.5023	-1.1685
0.60	0.9824	-0.7506	-0.7097
0.64	0.9087	-0.9145	-0.2277
0.68	0.8239	-0.9969	0.1999
0.72	0.7316	-1.0074	0.5221
0.76	0.6339	-0.9578	0.7212
0.80	0.5323	-0.8598	0.7977
0.84	0.4283	-0.7252	0.7649
0.88	0.3224	-0.5637	0.6452
0.92	0.2155	-0.3844	0.4620
0.96	0.1079	-0.1945	0.2399
1.00	0.0000	0.0000	0.0000

Table 13

MODE SHAPE ORDINATES -- FIRST THREE MODES

Parabolic Taper - Symmetric Beam - Depth Ratio $\mathcal{T} = 2.2$

$\eta = \frac{x}{l}$	First Mode Shape Ordinate	Second Mode Shape Ordinate	Third Mode Shape Ordinate
0.00	0.0000	0.0000	0.0000
0.04	0.1128	0.2007	0.2604
0.08	0.2253	0.3971	0.5038
0.12	0.3368	0.5829	0.7070
0.16	0.4466	0.7495	0.8411
0.20	0.5535	0.8859	0.8756
0.24	0.6558	0.9792	0.7844
0.28	0.7516	1.0161	0.5557
0.32	0.8382	0.9847	0.2011
0.36	0.9128	0.8774	-0.2368
0.40	0.9723	0.6946	-0.6859
0.44	1.0138	0.4466	-1.0572
0.48	1.0352	0.1542	-1.2679
0.52	1.0352	-0.1542	-1.2679
0.56	1.0138	-0.4466	-1.0572
0.60	0.9723	-0.6946	-0.6859
0.64	0.9128	-0.8774	-0.2368
0.68	0.8382	-0.9847	0.2011
0.72	0.7516	-1.0161	0.5557
0.76	0.6558	-0.9792	0.7844
0.80	0.5535	-0.8859	0.8756
0.84	0.4466	-0.7495	0.8411
0.88	0.3368	-0.5829	0.7070
0.92	0.2253	-0.3971	0.5038
0.96	0.1128	-0.2007	0.2604
1.00	0.0000	00.0000	0.0000

Table 14

MODE SHAPE ORDINATES -- FIRST THREE MODES

Parabolic Taper - Symmetric Beam - Depth Ratio $\tau = 3.0$

$\eta = \frac{x}{l}$	First Mode Shape Ordinate	Second Mode Shape Ordinate	Third Mode Shape Ordinate
0.00	0.0000	0.0000	0.0000
0.04	0.1096	0.1871	0.2262
0.08	0.2190	0.3717	0.4415
0.12	0.3280	0.5494	0.6291
0.16	0.4359	0.7141	0.7653
0.20	0.5420	0.8563	0.8205
0.24	0.6451	0.9638	0.7632
0.28	0.7432	1.0214	0.5677
0.32	0.8340	1.0125	0.2278
0.36	0.9140	0.9228	-0.2284
0.40	0.9793	0.7455	-0.7285
0.44	1.0258	0.4867	-1.1636
0.48	1.0501	0.1694	-1.4187
0.52	1.0501	-0.1694	-1.4187
0.56	1.0258	-0.4867	-1.1636
0.60	0.9793	-0.7455	-0.7285
0.64	0.9140	-0.9228	-0.2284
0.68	0.8340	-1.0125	0.2278
0.72	0.7432	-1.0214	0.5677
0.76	0.6451	-0.9638	0.7632
0.80	0.5420	-0.8563	0.8205
0.84	0.4359	-0.7141	0.7653
0.88	0.3280	-0.5494	0.6291
0.92	0.2190	-0.3717	0.4415
0.96	0.1096	-0.1871	0.2263
1.00	0.0000	0.0000	0.0000

Table 15

MODE SHAPE ORDINATES -- FIRST THREE MODES

Linear Taper - Unsymmetric Beam - Depth Ratio $\tau = 2.2$

$\eta = \frac{x}{l}$	First Mode Shape Ordinate	Second Mode Shape Ordinate	Third Mode Shape Ordinate
0.00	0.0000	0.0000	0.0000
0.04	0.1037	0.1791	0.2634
0.08	0.2066	0.3510	0.5024
0.12	0.3079	0.5086	0.6925
0.16	0.4067	0.6442	0.8111
0.20	0.5020	0.7504	0.8410
0.24	0.5928	0.8200	0.7738
0.28	0.6778	0.8472	0.6107
0.32	0.7559	0.8280	0.3643
0.36	0.8257	0.7599	0.0581
0.40	0.8860	0.6432	-0.2734
0.44	0.9355	0.4805	-0.5882
0.48	0.9728	0.2778	-0.8425
0.52	0.9966	0.0444	-0.9964
0.56	1.0057	-0.2076	-1.0185
0.60	0.9990	-0.4636	-0.8922
0.64	0.9755	-0.7069	-0.6208
0.68	0.9343	-0.9191	-0.2326
0.72	0.8748	-1.0814	0.2210
0.76	0.7969	-1.1767	0.6715
0.80	0.7008	-1.1915	1.0426
0.84	0.5873	-1.1165	1.2595
0.88	0.4577	-0.9481	1.2623
0.92	0.3142	-0.6920	1.0252
0.96	0.1600	-0.3657	0.5657
1.00	0.0000	0.0000	0.0000

Table 16

MODE SHAPE ORDINATES -- FIRST THREE MODES

Linear Taper - Unsymmetric Beam - Depth Ratio $\tau = 3.0$

$\eta = \frac{x}{l}$	First Mode Shape Ordinate	Second Mode Shape Ordinate	Third Mode Shape Ordinate
0.00	0.0000	0.0000	0.0000
0.04	0.0975	0.1604	0.2388
0.08	0.1945	0.3154	0.4586
0.12	0.2904	0.4591	0.6392
0.16	0.3844	0.5855	0.7605
0.20	0.4758	0.6881	0.8063
0.24	0.5637	0.7604	0.7669
0.28	0.6472	0.7966	0.6393
0.32	0.7252	0.7920	0.4289
0.36	0.7965	0.7433	0.1516
0.40	0.8598	0.6484	-0.1653
0.44	0.9141	0.5076	-0.4850
0.48	0.9578	0.3242	-0.7665
0.52	0.9894	0.1047	-0.9685
0.56	1.0074	-0.1415	-1.0524
0.60	1.0104	-0.4022	-0.9882
0.64	0.9969	-0.6617	-0.7639
0.68	0.9654	-0.9010	-0.3943
0.72	0.9145	-1.0983	0.0783
0.76	0.8431	-1.2327	0.5881
0.80	0.7506	-1.2846	1.0512
0.84	0.6369	-1.2369	1.3698
0.88	0.5023	-1.0767	1.4466
0.92	0.3482	-0.8019	1.2184
0.96	0.1785	-0.4294	0.6992
1.00	0.0000	0.0000	0.0000

Table 17

MODE SHAPE ORDINATES -- FIRST THREE MODES

Parabolic Taper - Unsymmetric Beam - Depth Ratio $\mathcal{T} = 2.2$

$\eta = \frac{x}{l}$	First Mode Shape Ordinate	Second Mode Shape Ordinate	Third Mode Shape Ordinate
0.00	0.0000	0.0000	0.0000
0.04	0.1006	0.1650	0.2381
0.08	0.2007	0.3251	0.4581
0.12	0.2998	0.4747	0.6406
0.16	0.3971	0.6073	0.7647
0.20	0.4918	0.7157	0.8115
0.24	0.5829	0.7924	0.7672
0.28	0.6692	0.8303	0.6265
0.32	0.7495	0.8233	0.3954
0.36	0.8222	0.7667	0.0924
0.40	0.8859	0.6585	-0.2506
0.44	0.9388	0.4996	-0.5901
0.48	0.9792	0.2949	-0.8758
0.52	1.0056	0.0537	-1.0579
0.56	1.0161	-0.2109	-1.0960
0.60	1.0096	-0.4814	-0.9681
0.64	0.9847	-0.7376	-0.6780
0.68	0.9407	-0.9578	-0.2593
0.72	0.8774	-1.1209	0.2261
0.76	0.7950	-1.2088	0.6965
0.80	0.6946	-1.2087	1.0650
0.84	0.5777	-1.1150	1.2570
0.88	0.4466	-0.9310	1.2279
0.92	0.3043	-0.6690	0.9744
0.96	0.1542	-0.3497	0.5384
1.00	0.0000	0.0000	0.0000

Table 18

MODE SHAPE ORDINATES -- FIRST THREE MODES

Parabolic Taper - Unsymmetric Beam - Depth Ratio $\tau = 3.0$

$\eta = \frac{x}{l}$	First Mode Shape Ordinate	Second Mode Shape Ordinate	Third Mode Shape Ordinate
0.00	0.0000	0.0000	0.0000
0.04	0.0937	0.1412	0.2067
0.08	0.1871	0.2792	0.4011
0.12	0.2799	0.4103	0.5689
0.16	0.3717	0.5297	0.6938
0.20	0.4617	0.6318	0.7586
0.24	0.5494	0.7103	0.7487
0.28	0.6339	0.7585	0.6538
0.32	0.7141	0.7699	0.4713
0.36	0.7887	0.7383	0.2086
0.40	0.8563	0.6589	-0.1138
0.44	0.9153	0.5291	-0.4619
0.48	0.9638	0.3494	-0.7892
0.52	0.9999	0.1245	-1.0420
0.56	1.0214	-0.1361	-1.1670
0.60	1.0262	-0.4175	-1.1219
0.64	1.0125	-0.6995	-0.8872
0.68	0.9784	-0.9578	-0.4774
0.72	0.9228	-1.1657	0.0537
0.76	0.8451	-1.2975	0.6166
0.80	0.7455	-1.3317	1.0999
0.84	0.6252	-1.2550	1.3948
0.88	0.4867	-1.0656	1.4227
0.92	0.3333	-0.7750	1.1602
0.96	0.1694	-0.4081	0.6509
1.00	0.0000	0.0000	0.0000

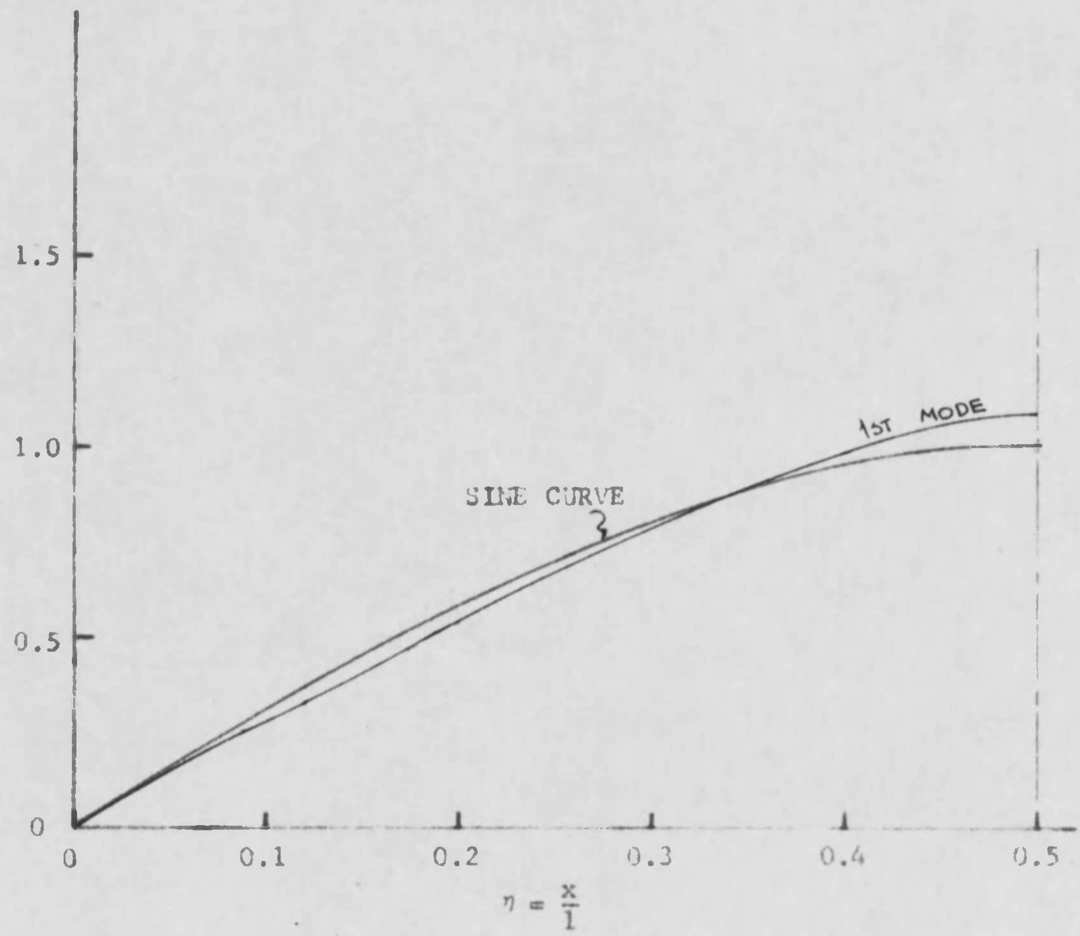

Fig . 17

FIRST MODE - SINE CURVE

Linear Taper - Symmetric Beam - Depth Ratio $\tau = 3.0$

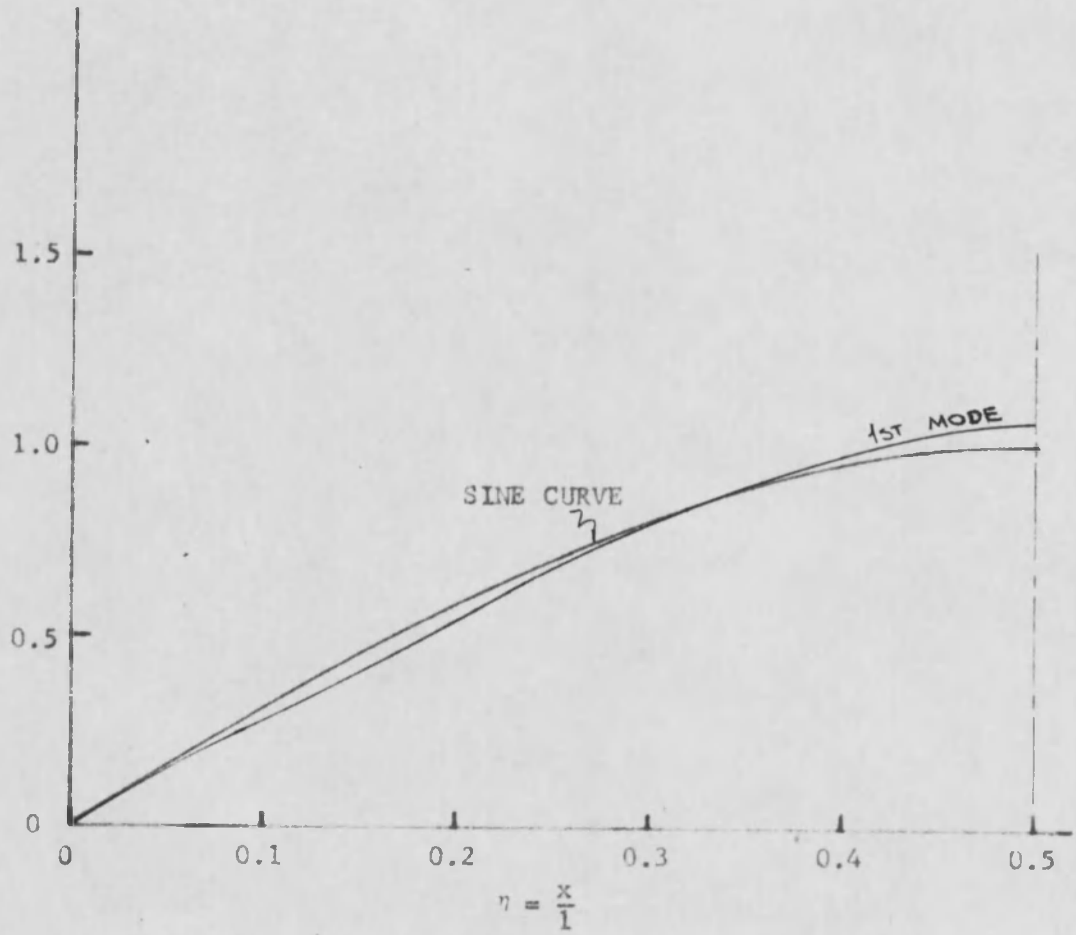

Fig. 18

FIRST MODE - SINE CURVE

Parabolic Taper - Symmetric Beam - Depth Ratio $\tau = 3.0$

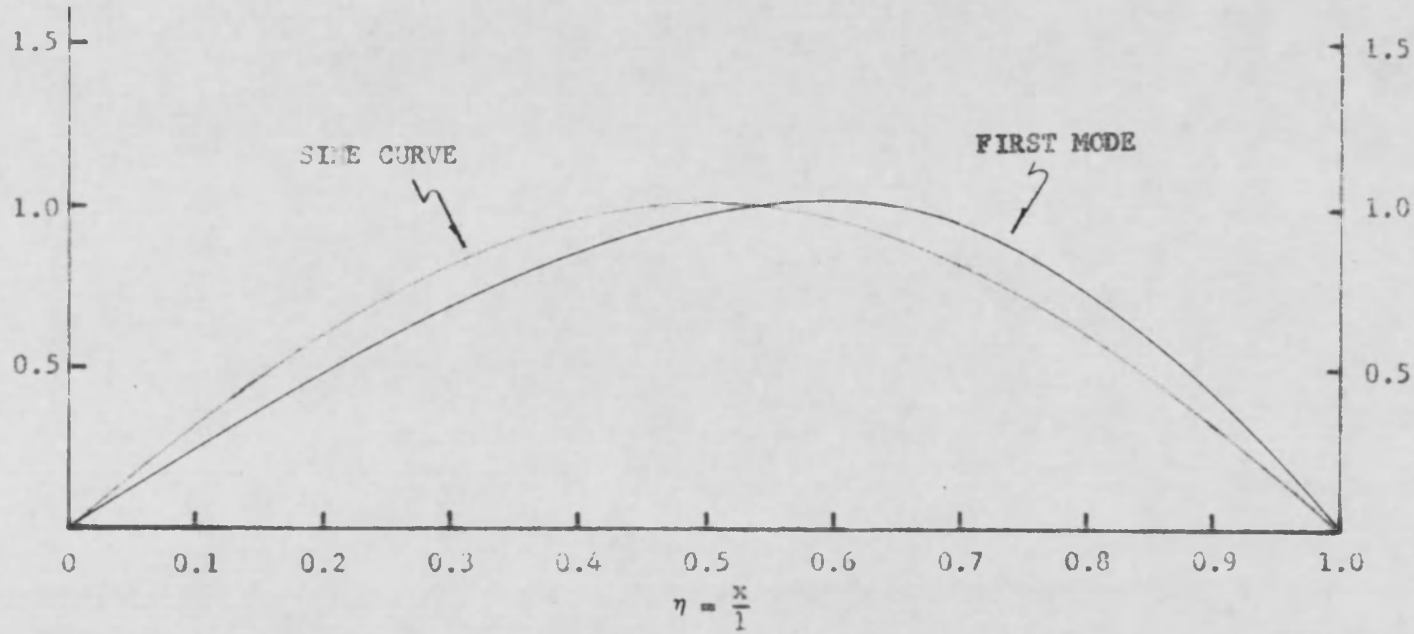

Fig. 19

FIRST MODE - SINE CURVE

Linear Taper - Unsymmetric Beam - Depth Ratio $\tau = 3.0$

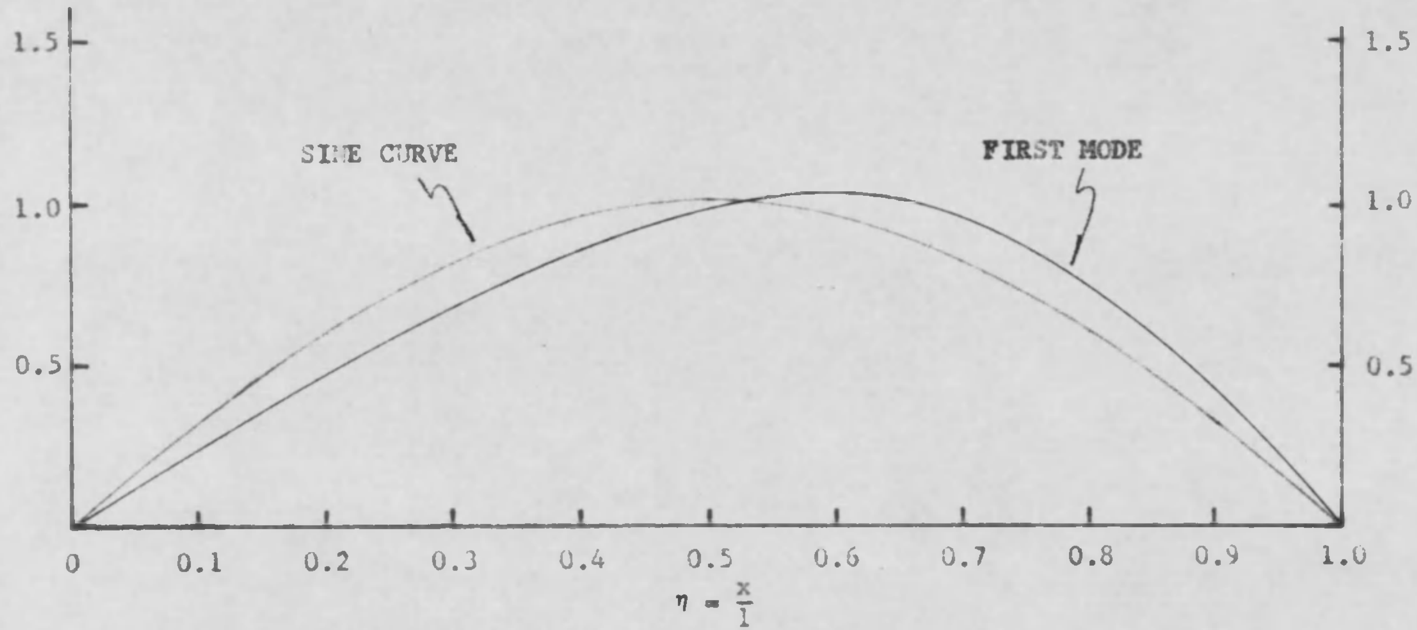

Fig. 20

FIRST MODE - SINE CURVE

Parabolic Taper - Unsymmetric Beam - Depth Ratio $\tau = 3.0$

fundamental sine curve. Only a depth ratio of 3.0 was considered as this depth ratio resulted in the greatest distortion.

Tables 19 and 20 indicate changes in the frequency ratios as the number of equations (85) was increased from twenty to fifty. This comparison was necessary as convergence of the iterative process did not necessarily indicate convergence to the exact solution. Equations were added until negligible changes in the b_k^i coefficients occured. Tables 19 and 20 indicate that solutions using the first twenty equations yield low-error approximations to the low order mode shapes and natural frequencies.

Table 19

FREQUENCY RATIO VARIATIONS

Linear Taper - Symmetric Beam - Depth Ratio $T = 2.2$

Terms in Series	$\frac{\omega_1}{\omega_{o1}}$	$\frac{\omega_3}{\omega_{o3}}$	$\frac{\omega_5}{\omega_{o5}}$
10	1.25004	1.54656	1.54568
15	1.24983	1.54637	1.54545
20	1.24978	1.54634	1.54540
25	1.24977	1.54633	1.54539
Percent Change Between 10 and 25 Terms	0.022	0.015	0.019

Table 20

FREQUENCY RATIO VARIATIONS

Linear Taper - Symmetric Beam - Depth Ratio $\tau = 3.0$

Terms in Series	$\frac{\omega_1}{\omega_{o1}}$	$\frac{\omega_2}{\omega_{o2}}$	$\frac{\omega_3}{\omega_{o3}}$	$\frac{\omega_4}{\omega_{o4}}$	$\frac{\omega_5}{\omega_{o5}}$	$\frac{\omega_6}{\omega_{o6}}$
10	1.35233	1.82232	1.90013	1.89626	1.88370	1.88537
15	1.35140	1.82224	1.89936	1.89602	1.88267	1.88488
20	1.35117	1.82224	1.89920	1.89601	1.88247	1.88483
25	1.35110	1.82224	1.89916	1.89601	1.88242	1.88482
Percent Change Between 10 and 25 Terms	0.091	0.005	0.052	0.014	0.078	0.030

EXPERIMENTAL RESULTS

An experimental model was made and a test performed in an attempt to verify the theoretical results.

An aluminum beam was milled with a parabolic variation to a depth ratio of 2.21 - see Appendix D for calculations. The beam length was sixty inches and the width and maximum depth were one inch.

The beam was simply-supported and set in motion in an attempt to simulate the first mode of vibration. A Sanborne chart recorder was used to record the strain variation at the beam center. Peaks through a given time interval were counted, and the first natural frequency was determined experimentally as 77.82 radians per second. This compares to the 77.43 radians per second calculated from Figure 6.

The error of 0.6% indicates that the theoretical equations developed will likely yield extremely low-error results for the low-order natural frequencies.

CONTENTS OF THE APPENDICES

The contents of the respective appendices are as follows:

Appendix A -- development of c_{rs} and d_{rs} for simply-supported beams.

Appendix B -- mass distribution, stiffness, and evaluation of the c_{rs} and d_{rs} integrals for the linear and parabolic tapered beams.

Appendix C -- development of equations for the unsymmetric beams.

Appendix D -- example of calculation using frequency ratio-depth ratio curve for the experimental beam.

Appendix E -- the flow diagram and print-out sheet for the iteration routine.

APPENDIX A

The c_{rs} and d_{rs} equations are:

$$c_{rs} = \int_0^l m\bar{\phi}_r\bar{\phi}_s\,dx \quad \text{and} \qquad (A-1)$$

$$d_{rs} = \int_0^l EI\bar{\phi}_r''\bar{\phi}_s''\,dx \qquad (A-2)$$

Using Jones'[(7)] technique, the $\bar{\phi}_r$ functions for a simply-supported beam are

$$\bar{\phi}_r = \sin\frac{r\pi x}{l} \qquad (A-3)$$

Therefore, the c_{rs} and d_{rs} equations are

$$c_{rs} = \int_0^l m \sin\frac{r\pi x}{l}\sin\frac{s\pi x}{l}\,dx \quad \text{and} \qquad (A-4)$$

$$d_{rs} = (rs)^2\frac{\pi^4}{l^4}\int_0^l EI \sin\frac{r\pi x}{l}\sin\frac{s\pi x}{l}\,dx \qquad (A-5)$$

where the evaluation of the above integrals depends on the forms of the mass(m) and stiffness(EI) functions.

APPENDIX B

I. Linear Taper

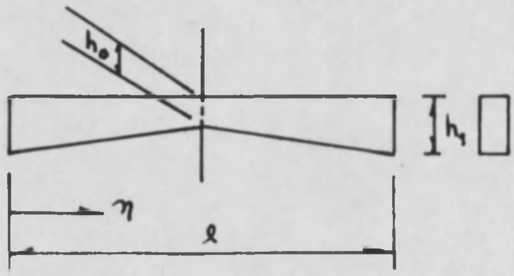

Depth Ratio $\tau = h_1/h_o$

Fig. A-1

A. Mass Distribution

$$m = m_o[\tau + 2(1-\tau)\eta] \tag{A-6}$$

$$0 \leq \eta \leq 1/2$$

B. Stiffness

$$EI = EI_o[8(1-\tau)^3\eta^3 + 12\tau(1-\tau)^2\eta^2 + 6\tau^2(1-\tau)\eta + \tau^3] \tag{A-7}$$

$$0 \leq \eta \leq 1/2$$

C. Coefficients: all c_{rs} and d_{rs} coefficients are zero for $(r \pm s)$ equal to an odd number. For $(r \pm s)$ equal to an even number:

1. $$c_{rs} = 2m_o(1-\tau)\left[\frac{(-1)^{\frac{r-s}{2}}}{(r-s)^2\pi^2} - \frac{(-1)^{\frac{r+s}{2}}}{(r+s)^2\pi^2} - \frac{-1}{(r-s)^2\pi^2} + \frac{1}{(r+s)^2\pi^2}\right] \qquad \text{(A-8)}$$

$$r \neq s$$

2. $$c_{rr} = m_o\left[0.50\tau + (1-\tau)\left(\frac{1}{4} + \frac{1}{2r^2\pi^2} - \frac{(-1)^r}{2r^2\pi^2}\right]\right. \qquad \text{(A-9)}$$

3. $$d_{rs} = \frac{EI_o\pi^4}{\ell^4}\left[(rs)^2\right]\left[8(1-\tau)^3\left\{\left(\frac{3}{4\pi^2(r-s)^2} - \frac{6}{(r-s)^4\pi^4}\right)(-1)^{\frac{r-s}{2}} + \left(\frac{-3}{4\pi^2(r+s)^2} + \frac{6}{(r+s)^4\pi^4}\right)(-1)^{\frac{r+s}{2}} + \frac{6}{(r-s)^4\pi^4} - \frac{6}{(r+s)^4\pi^4}\right\} + 12\tau(1-\tau)^2\left\{\frac{(-1)^{\frac{r-s}{2}}}{(r-s)^2\pi^2} - \frac{(-1)^{\frac{r+s}{2}}}{(r+s)^2\pi^2}\right\} + 6\tau^2(1-\tau)\left\{\frac{(-1)^{\frac{r-s}{2}}}{(r-s)^2\pi^2} - \frac{(-1)^{\frac{r+s}{2}}}{(r+s)^2\pi^2} - \frac{1}{(r-s)^2\pi^2} + \frac{1}{(r+s)^2\pi^2}\right\}\right] \qquad \text{(A-10)}$$

$$r \neq s$$

$$4.\quad d_{rr} = \frac{EI_o\pi^4}{\ell^4}\left[r^4\right]\left[0.50(1-\tau)^3\left\{\frac{1}{4} - \frac{6}{r^4\pi^4} - \frac{3(-1)^r}{r^2\pi^2} + \frac{6(-1)^r}{r^4\pi^4}\right\} + 1.50\,\tau(1-\tau)^2\cdot\left\{\frac{1}{3} - \frac{2(-1)^r}{r^2\pi^2}\right\} + 1.50\,\tau^2(1-\tau)\left\{\frac{1}{2} + \frac{1}{r^2\pi^2} - \frac{(-1)^r}{r^2\pi^2}\right\} + 0.50\,\tau^3\right]$$

(A-11)

II. Parabolic Taper

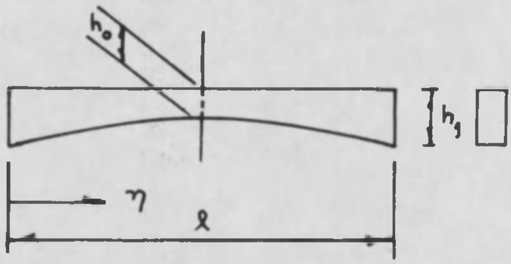

Depth Ratio $\tau = h_1/h_o$

Fig. A-2

A. Mass Distribution

$$m = m_o\left[\tau + 4(\tau-1)\eta^2 - 4(\tau-1)\eta\right]$$

$$0 \le \eta \le 1 \qquad \text{(A-12)}$$

B. Stiffness

$$\begin{aligned} EI = EI_o\big[&64(\tau-1)^3\eta^6 - 192(\tau-1)^3\eta^5 + \\ &48(\tau-1)^2(5\tau-4)\eta^4 - 32(\tau-1)^2(5\tau-2)\eta^3 + \\ &12\tau(\tau-1)(5\tau-4)\eta^2 - 12\tau^2(\tau-1)\eta + \tau^3\big] \end{aligned}$$

$$0 \le \eta \le 1 \qquad \text{(A-13)}$$

C. Coefficients: all c_{rs} and d_{rs} coefficients are zero for $(r \pm s)$ equal to an odd number. For $(r \pm s)$ equal to an even number:

1. $$c_{rs} = 4m_o(\tau-1)\left\{\frac{1}{(r-s)^2\pi^2} - \frac{1}{(r+s)^2\pi^2}\right\}$$

$$r \ne s \qquad \text{(A-14)}$$

$$2.\quad c_{rr} = m_o\left[0.50\,\tau + (1-\tau)\left(\frac{1}{3} - \frac{1}{r^2\pi^2}\right)\right]$$

(A-15)

$$3.\quad d_{rs} = \frac{EI_o\pi^4}{\ell^4}\left[(rs)^2\right]\left[64(\tau-1)^3\left\{\left(\frac{3}{16(r-s)^2\pi^2} - \right.\right.\right.$$

$$\left.\frac{15}{(r-s)^4\pi^4} + \frac{360}{(r-s)^6\pi^6}\right)(-1)^{\frac{r-s}{2}} + \left(\frac{-3}{16(r+s)^2\pi^2} + \right.$$

$$\left.\left.\frac{15}{(r+s)^4\pi^4} - \frac{360}{(r+s)^6\pi^6}\right)(-1)^{\frac{r+s}{2}}\right\} - 192(\tau-1)^3\cdot$$

$$\left\{\left(\frac{5}{16(r-s)^2\pi^2} - \frac{15}{(r-s)^4\pi^4} + \frac{120}{(r-s)^6\pi^6}\right)(-1)^{\frac{r-s}{2}} + \right.$$

$$\left(\frac{5}{16(r+s)^2\pi^2} + \frac{15}{(r+s)^4\pi^4} - \frac{120}{(r+s)^6\pi^6}\right)(-1)^{\frac{r+s}{2}} +$$

$$\left.\frac{120}{(r+s)^6\pi^6} - \frac{120}{(r-s)^6\pi^6}\right\} + 48(\tau-1)^2(5\tau-4)\cdot$$

$$\left\{\left(\frac{1}{2(r-s)^2\pi^2} - \frac{12}{(r-s)^4\pi^4}\right)(-1)^{\frac{r-s}{2}} + \left(\frac{-1}{2(r+s)^2\pi^2} + \right.\right.$$

$$\left.\left.\frac{12}{(r+s)^4\pi^4}\right)(-1)^{\frac{r+s}{2}}\right\} - 32(\tau-1)^2(5\tau-2)\cdot$$

$$\left\{\frac{3}{4}(r-s)^2\pi^2 - \frac{6}{(r-s)^4\pi^4}\right)(-1)^{\frac{r-s}{2}} + \left(\frac{-3}{4(r+s)^2\pi^2} + \right.$$

$$\frac{6}{(r+s)^4\pi^4}\Big)(-1)^{\frac{r+s}{2}} + \frac{6}{(r-s)^4\pi^4} - \frac{6}{(r+s)^4\pi^4}\Big\} +$$

$$12\tau(\tau-1)(5\tau-4)\left\{\frac{(-1)^{\frac{r-s}{2}}}{(r-s)^2\pi^2} - \frac{(-1)^{\frac{r+s}{2}}}{(r+s)^2\pi^2}\right\} -$$

$$12\tau^2(\tau-1)\left\{\frac{(-1)^{\frac{r-s}{2}}}{(r-s)^2\pi^2} - \frac{(-1)^{\frac{r+s}{2}}}{(r+s)^2\pi^2} - \frac{1}{(r-s)^2\pi^2} +\right.$$

$$\left.\frac{1}{(r+s)^2\pi^2}\right\}\Bigg] \qquad r \neq s \tag{A-16}$$

4. $$d_{rr} = \frac{EI_o\pi^4}{\ell^4}\left[r^4\right]\Bigg[0.50(\tau-1)^3\left\{\frac{1}{7} + \left(\frac{-6}{r^2\pi^2} +\right.\right.$$

$$\left.\left.\frac{120}{r^4\pi^4} - \frac{720}{r^6\pi^6}\right)(-1)^r\right\} - 3(\tau-1)^3\left\{\frac{1}{6} +\right.$$

$$\left.\frac{120}{r^6\pi^6} + \left(\frac{-5}{r^2\pi^2} + \frac{60}{r^4\pi^4} - \frac{120}{r^6\pi^6}\right)(-1)^r\right\} +$$

$$1.50(\tau-1)^2(5\tau-4)\left\{\frac{1}{5} + \left(\frac{-4}{r^2\pi^2} +\right.\right.$$

$$\left.\left.\frac{24}{r^4\pi^4}\right)(-1)^r\right\} - 2(\tau-1)^2(5\tau-2)\left\{\frac{1}{4} -\right.$$

$$\left.\frac{6}{r^4\pi^4} + \left(\frac{-3}{r^2\pi^2} + \frac{6}{r^4\pi^4}\right)(-1)^r\right\} +$$

$$1.50\,\tau(\tau-1)(5\tau-4)\left\{\frac{1}{3} - \frac{2(-1)^r}{r^2\pi^2}\right\} -$$

$$3\tau^2(\tau-1)\left\{\frac{1}{2} + \frac{1}{r^2\pi^2} - \frac{(-1)^r}{r^2\pi^2}\right\} +$$

$$0.50\,\tau^3\Big] \qquad \text{(A-17)}$$

APPENDIX C

This appendix indicates how the frequencies and mode shapes of the unsymmetric beams are related to those of the symmetric beams.

The Rayleigh-Ritz equations for the unsymmetric beams are of the form:

$$\omega_{\upsilon}^{2}\sum_{r'=1}^{\infty} b_{r'}\int_{0}^{l'} m\bar{\phi}_{r'}\bar{\phi}_{s'}dx - \sum_{r'=1}^{\infty} b_{r'}\int_{0}^{l'} EI\bar{\phi}_{r'}''\bar{\phi}_{s'}''dx = 0 \qquad \text{(A-18)}$$

$$s' = 1, 2, \ldots \infty$$

where l' is the length of the unsymmetric beam.

In terms of the length(l) of the symmetric beams, l' is

$$l' = \frac{l}{2} \qquad \text{(A-19)}$$

Therefore, the $\bar{\phi}_{r'}$ functions for the unsymmetric beams are

$$\bar{\phi}_{r'} = \sin \frac{2r'\pi x}{l} \qquad \text{(A-20)}$$

Substituting the $\bar{\phi}_{r'}$ functions into the Rayleigh-Ritz equations gives

$$\omega_u^2 \sum_{r'=1}^{\infty} b_{r'} \int_0^{1/2} m \cdot \sin 2r'\pi\eta \cdot \sin 2s'\pi\eta \; d\eta \; -$$

$$\frac{16\pi^4}{l^4} \sum_{r'=1}^{\infty} b_{r'} (r's')^2 \int_0^{1/2} EI \cdot \sin 2r'\pi\eta \cdot \sin 2s'\pi\eta \; d\eta \; = \; 0 \qquad \text{(A-21)}$$

$$s' = 1, 2, 3, \ldots \infty$$

where the u subscript denotes the frequency for the unsymmetric beam.

For the unsymmetric case

$$\omega_u'^2 = \frac{16\pi^4 EI_o}{l^4 M_o} \qquad \text{(A-22)}$$

and substituting for EI and A, the square of the natural frequency for the unsymmetric beam is

$$\omega_u^2 = \omega_u'^2 \frac{\sum_{r'=1}^{\infty} b_{r'} r'^2 s'^2 \int_0^{1/2} \psi(x) \sin 2r'\pi\eta \cdot \sin 2s'\pi\eta \; d\eta}{\sum_{r'=1}^{\infty} b_{r'} \int_0^{1/2} \rho(x) \sin 2r'\pi\eta \cdot \sin 2s'\pi\eta \; d\eta} \qquad \text{(A-23)}$$

$$s' = 1, 2, 3, \ldots \infty$$

The corresponding equation for the natural frequency for the symmetric beam is

$$\omega^2 = \frac{\omega'^2 \sum_{r=1}^{\infty} b_r (rs)^2 \int_0^{1/2} \psi(x) \sin r\pi\eta \cdot \sin s\pi\eta \, d\eta}{\sum_{r=1}^{\infty} b_r \int_0^{1/2} \rho(x) \sin r\pi\eta \cdot \sin s\pi\eta \, d\eta} \qquad \text{(A-24)}$$

$$s = 1, 2, 3, \ldots \infty$$

For the unsymmetric beam, the square of the natural frequency for a uniform beam is

$$\omega^2_{ouk'} = \frac{16k'^4 \pi^4 EI_o}{l^4 \cdot M_o} \qquad \text{(A-25)}$$

The corresponding equation for the symmetric beam is

$$\omega^2_{ok} = \frac{k^4 \pi \; EI_o}{l^4 \cdot M_o} \qquad \text{(A-26)}$$

Therefore, the values of the frequency ratios, $\frac{\omega_k}{\omega_{ok}}$ and $\frac{\omega_{uk'}}{\omega_{ouk'}}$, for the symmetric and unsymmetric beams will be equal when k' is one and k is two, when k' is two and k is four, and when k' is three and k is six, ...

APPENDIX D

The experimental beam used was

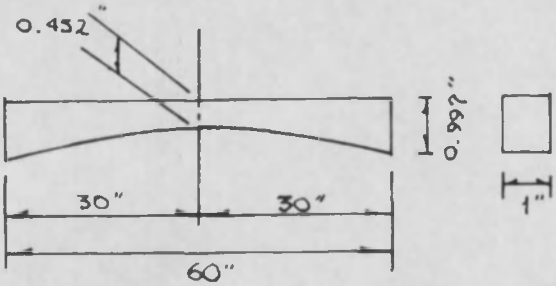

Fig. A-3

$$\text{Depth Ratio } \tau = \frac{0.997}{0.452} = 2.21 \tag{A-27}$$

From Fig. 6, the frequency ratio for the first mode shape is

$$\frac{\omega_1}{\omega_{01}} = 1.09 \tag{A-28}$$

Therefore,

$$\omega_1 = 1.09 \frac{\pi^2}{1^2} \sqrt{\frac{EI_o}{M_o}} \tag{A-29}$$

From calculations

$$\omega_{01} = \frac{100\pi^2}{36} \sqrt{6.7128} = 7.197\pi^2 \text{ radians/second} \tag{A-30}$$

therefore,

$$\underline{\omega_1 = 77.43 \text{ radians/second}} \tag{A-31}$$

APPENDIX E

The equations used in the iteration scheme were put in the form:

$$\sum_{j=1}^{n}(b_{ij} - y a_{ij})x_j = 0 \qquad \text{(A-32)}$$

$i = 1,2,3, \ldots n$ where

$$y = \frac{\omega^2}{\omega_o^2} \quad ; \quad \omega_o^2 = \pi^4 l^4 \frac{EI_o}{m_o} \quad ; \qquad \text{(A-33) \& (A-34)}$$

$$b_{ij} = \frac{1}{\pi^4}\int_0^1 \psi(\eta)\,\bar{\phi}_i''(\eta)\,\bar{\phi}_j''(\eta)\,d\eta \quad ; \qquad \text{(A-35)}$$

$$a_{ij} = \int_0^1 \rho(\eta)\,\bar{\phi}_i(\eta)\,\bar{\phi}_j(\eta)\,d\eta \quad ; \qquad \text{(A-36)}$$

$\bar{\phi}_i(\eta)$ = the i th mode shape of the uniform beam.

and

n = number of equations, also equals the number of terms from the series expansion.

k_{max} = number of values of y that are desired; $k_{max} \leq n$

E_T = test number to determine when iteration is to be stopped.

I = number of cycles of iteration; $I \leq 100$.

E_y = difference between y when iteration is stopped, and the value of y from the preceeding iteration.

$E = \sum \left| x_i^s - x_i^{s-1} \right|$ where: $x_i^s = x_i$ at the end of s iterations
$x_i^{s-1} = x_i$ at the end of s-1 iterations.

c, x_s, y_s are used for temporary storage.

Flow diagram for iteration to determine the frequencies and mode shapes:

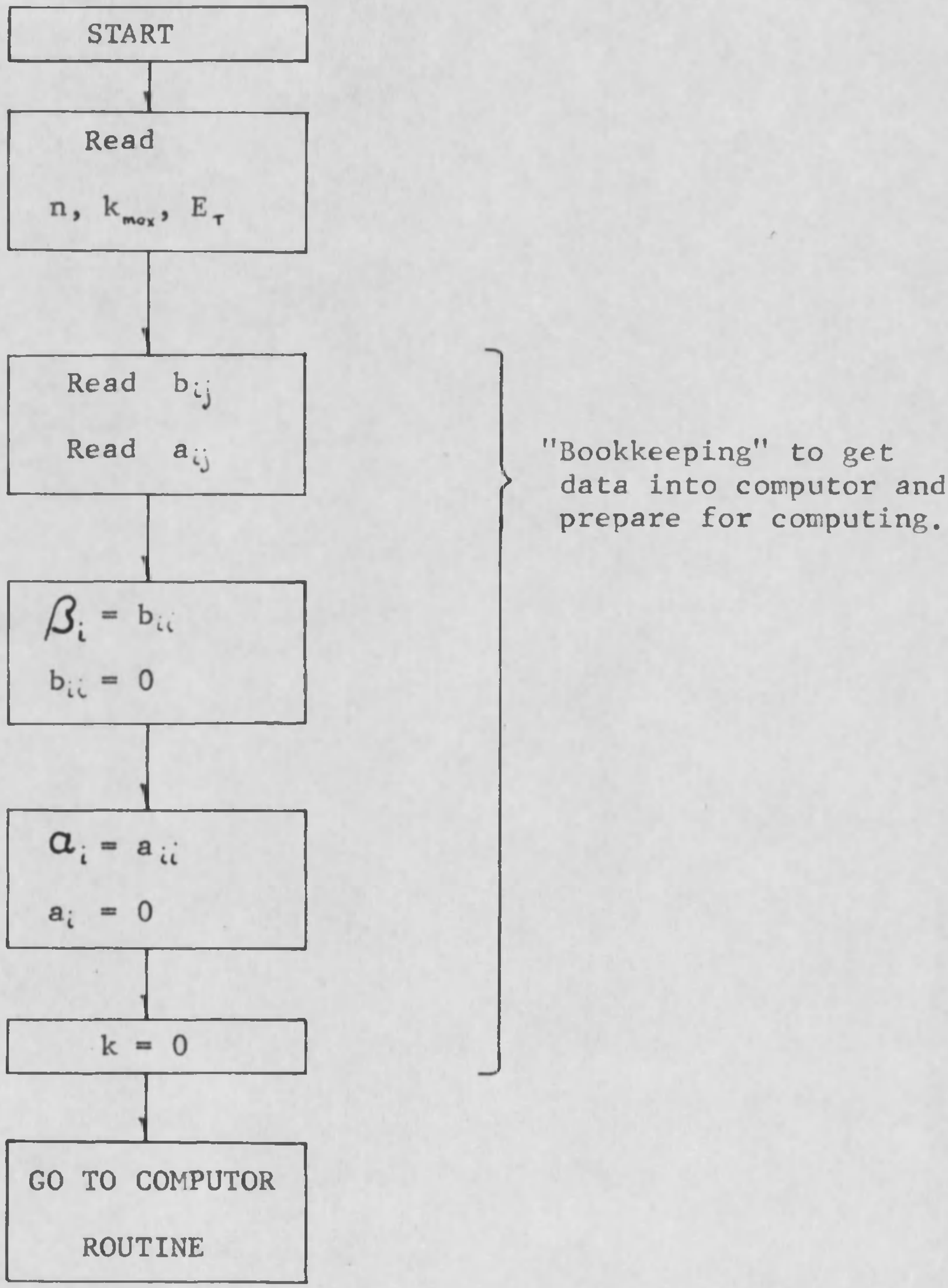

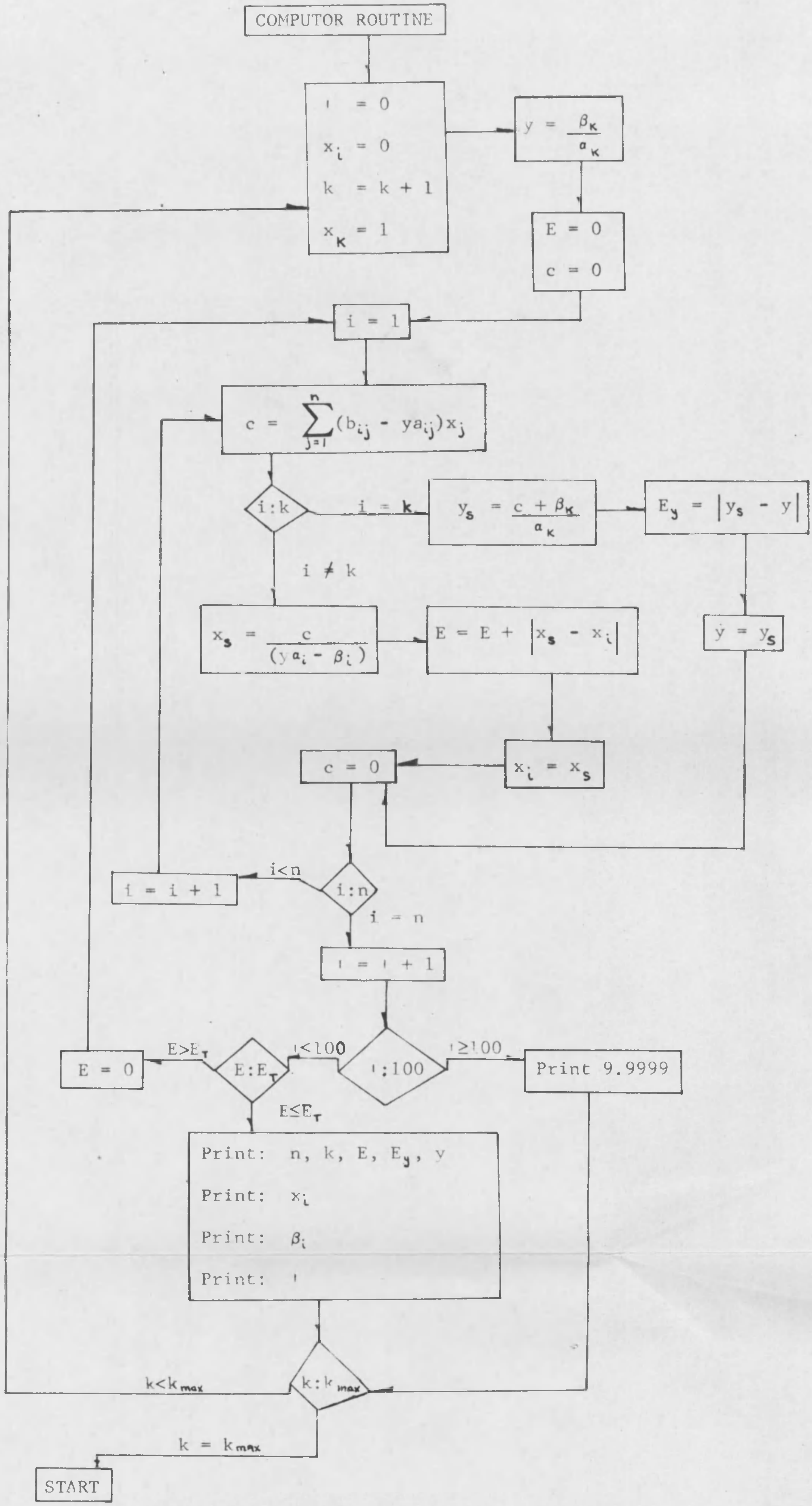
COMPUTOR ROUTINE
i = 0
x_i = 0
k = k + 1
x_K = 1
y = β_K / a_K
E = 0
c = 0
i = 1
c = $\sum_{j=1}^{n} (b_{ij} - y a_{ij}) x_j$
i:k
i = k
$y_s = \frac{c + \beta_K}{a_K}$
$E_y = |y_s - y|$
i ≠ k
$x_s = \frac{c}{(y a_i - \beta_i)}$
E = E + $|x_s - x_i|$
y = y_s
$x_i = x_s$
c = 0
i<n
i = i + 1
i:n
i = n
i = i + 1
E>E_T
i<100
i≥100
E = 0
E:E_T
i:100
Print 9.9999
E≤E_T
Print: n, k, E, E_y, y
Print: x_i
Print: β_i
Print: i
k<k_{max}
k:k_{max}
k = k_{max}
START

PRINT-OUT OF ITERATION ROUTINE

```
        Dimension B(30,30),A(30,30 ),BT(30),AL(30) ,X(30)
2       Format (2I4,1PE14.5)
3       Format (1P5E14.5)
4       Format(2I4,1P3E14.5)
5       Format(1I4)
10      Read 2,N,KMAX,ET
        N=N
        Do 11 I=1,N
11      Read 3,(B(I,J),J=1,N)
        Do 12 I=1,N
12      Read 3,(A(I,J),J=1,N)
        Go to 25
25      Do 30 I=1,N
        BT(I)=B(I,I)
        B(I,I) = 0.
        AL(I) = A(I,I)
30      A(I,I) = 0.
        K = 0
35      L=0
        Do 40 I=1,N
40      X(I) =0.
        K=K+1
        X(K)=1.0
        Y=BT(K)/AL(K)
        E =0.
        C=0.
        Go to 45
45      Do 55I=1,N
46      Do 47 J=1,N
47      C=C+(B(I,J)-Y*A(I,J))*X(J)
        If(I-K)49,50,49
49      XS=C/(Y*AL(I)-BT(I))
        E=E+ABSF(XS-X(I))
        X(I) =XS
        Go to 54
50      YS=(C+BT(K))/AL(K)
        EY =ABSF(YS-Y)
        Y=YS
54      Continue
        C=0.
```

```
55      Continue
        L = L+1
60      If(100-L)85,65,65
65      If(E-ET)70,70,66
66      E=0.
        Go to 45
70      Go to 80
80      Print4,N,K,E,EY,Y
81      Print3,(X(I),I=1,N)
82      Print3,(BT(I),I=1,N)
83      Print 5,L
        If(K-KMAX)35,10,10
85      P=9.9999
        Print 3,P,P,P,P,P
```

BIBLIOGRAPHY

1. Cranch, E.T. and Alfred A. Adler, "Bending Vibrations of Variable Section Beams." Transactions of The American Society of Mechanical Engineers, Journal of Applied Mechanics, vol. 23, No. 1, March, 1956, p. 103.

2. Fertis, D.G. and E.C. Zobel, Transverse Vibration Theory, New York City, The Ronald Press, 1961.

3. Harris, Cyril M. and Charles E. Crede, Shock and Vibration Handbook, vol. I, New York City, The McGraw - Hill Co., 1961.

4. Housner, G.W. and W.O. Keightley, "Vibrations of Linearly Tapered Cantilever Beams. Proceedings of The American Society of Civil Engineers, Journal of the Engineering Mechanics Division, vol. 88, Em2, April, 1962, Part I, pp. 95-123.

5. Huang, T.C. and N.C. Wu, "Approximate Analysis of Flexural Vibrations of Beams." Engineering Progress at the University of Florida, Technical Paper Series, vol. XVI, No.2, February, 1962.

6. Jacobsen, L.S. and R.S. Ayre, Engineering Vibrations, New York City, The McGraw - Hill Co., 1958.

7. Jones, R.P.N. and S. Mahalingem, "The Natural Frequencies of Free and Constrained Non-Uniform Beams." Journal of The Royal Aeronautical Society, Nov., 1960, pp. 697-699

8. McLachlan, N.W., Theory of Vibrations, New York City, Dover Publications, 1951.

9. Myklestad, N.O., Fundamentals of Vibration Analysis, New York City, The McGraw - Hill Co., 1956.

10. Nicholson, J.W., "The Lateral Vibration of Bars of Variable Section." Proceedings of the Royal Society, Series A, vol. 93, No. A654, September 1, 1917, p. 506.

11. Rodgers, G.L., Dynamics of Framed Structures, New York City, John Wiley and Sons, 1959.

12. Timoshenko, S.P. and D.H. Young, Vibration Problems in Engineering, Third Edition, Princeton, New Jersey, D. Van Nostrand Co., January, 1955.

13. Timoshenko, S.P., "On the Corrections for Shear of the Differential Equation for Transverse Vibrations." _Philosophical Magazine and Journal of Sciences_, Series 6, vol. 43, 1921, pp. 744-746.